Enhanced Depolarized Electro-Membrane System (EDEMS) for Direct Capture of Carbon Dioxide from Ambient Air
Final Technical Report

Reporting Period:
October 1st, 2020 to March 31st, 2022

Principal Authors:
Ayokunle Omosebi, Xin Gao, Jesse Thompson, Jinwen Wang, Lisa Richburg, and Kunlei Liu

University of Kentucky, Lexington, KY

Report Issued
June 2022

Work Performed Under Award Number
DE-FE0031962

SUBMITTED BY
University of Kentucky Research Foundation
109 Kinkead Hall, Lexington, KY 40506-0057

PRINCIPAL INVESTIGATORS
Ayokunle Omosebi
p. 859-257-0346
f. 859-257-0302
Ayokunle.omosebi@uky.edu

U.S. DOE NETL PROGRAM MANAGER
Krista Hill
Krista.Hill@netl.doe.gov

SUBMITTED TO
U.S. Department of Energy National Energy Technology Laboratory

ACKNOWLEDGEMENT: UK CAER is grateful to the U.S Department of Energy National Energy Technology Laboratory for supporting this project.

ABSTRACT: The goal of this final project report is to summarize the work conducted on project DE-FE0031962. In accordance with the Statement of Project Objectives (SOPO), the University of Kentucky Center for Applied Energy Research (UK CAER) (Recipient) developed an intensified process to capture CO_2 from ambient conditions (400 ppm CO_2). The process combines low-temperature solvent-aided membrane capture with electrochemically-mediated solvent regeneration to simultaneously capture ambient CO_2 while regenerating the solvent. The technology employs only two primary units (regenerator and absorber/contactor) while generating high purity hydrogen as a co-product that can be sold, used for energy storage, or cost-saving depolarization of the direct air capture (DAC) system during the grid peak demand, allowing for flexible operation. When depolarization is employed, the operating voltage is reduced by more than 1 V. Since the technology is powered directly by DC electricity, it can seamlessly tie in with power sources like solar cells without the need for AC/DC converters, therefore allowing for a remote operation to further mitigate greenhouse gas generation toward deploying a negative carbon emissions technology that is completely decoupled from the carbon emissions from the power source for the DAC unit.

The project results verified that UK CAER's integrated approach addressed the complexities of incumbent DAC systems by demonstrating at ambient conditions, including (1) low gas-side pressure-drop facile CO_2 capture via a membrane contactor with in-situ generated hydroxide as capture solvent, (2) multi-functional electrochemical regenerator for hydroxide regeneration, CO_2 concentration and hydrogen production, and (3) depolarization using cathode-produced hydrogen to reduce energy requirement. The EH&S Assessment of the process did not identify any obvious concern for the bench-scale operation and no apparent barriers to implementing UK CAER's carbon capture and solvent regeneration system at a larger scale.

Table of Contents

1) EXECUTIVE SUMMARY

1.1 Overview

The major accomplishments of this project are highlighted below:

- Fabricated a low-pressure drop (<1 Pa cm^{-1}) tubular membrane contactor with > 2 mm internal diameter and demonstrated the contactor for effective direct air capture (DAC) facilitated by hydroxides.
- Demonstrated the stability of the hydrophobic agent coated membrane contactor under caustic conditions. The membranes can be refreshed with periodic drying.
- Achieved 25% area enhancement of the membrane contactor via a sandblasting approach and 137% via laser patterning.
- Tuned the regeneration capability of the electrochemical solvent regenerator to achieve pH swing using a combination of solvent concentration, flow rate, and operating current, with the variables lumped together as the loading factor.
- Achieved 100% hydrogen generation efficiency in the electrochemical solvent regenerator and demonstrated that hydrogen depolarization of the anode reduced the voltage requirement by ~1.2 V.
- DAC operation including the integrated MC and ERC at 0.5 A and <1.8 V achieved 60% CO_2 capture efficiency from 2 L/hr influent air (~5 s residence time), including a stable performance for over 40+ hours where the capture performance depended on the pH swing from 12.2 to 12.6.
- The EH&S Assessment of the process did not identify any obvious concerns for the bench-scale operation and no apparent barriers to implementing the DAC system at a larger scale.

The University of Kentucky Center for Applied Energy Research (UK CAER) developed an intensified process to capture CO_2 from ambient conditions (400 ppm CO_2). Using only a two-unit operation comprised of a membrane contactor (MC) and electrochemical regeneration cell (ERC), the UK CAER process couples low-temperature solvent-aided membrane capture with electrochemically-mediated solvent regeneration to simultaneously capture ambient CO_2 while regenerating the capture media. A key benefit of the technology is its capability for a seamless tie-in with direct current (DC) electricity power sources like solar cells without AC/DC converters for a remote operation to further mitigate greenhouse gas generation toward deploying a negative carbon emissions technology. Concurrently, the technology also generates hydrogen as a byproduct that can be sold to recuperate capture cost, used for energy storage and grid management, or used for cost-saving depolarization of the DAC system, therefore offering the flexibility for process integration with various existing applications. The technology was advanced during the project performance period from TRL 3 to 4 by demonstrating continuous operation with an integrated process using <3.5 V for solvent regeneration and maintaining >50% CO_2 capture from air influent at 2 L/hr for 40+ hours.

The membrane contactor and electrochemical reactor were independently developed before integrating them to demonstrate continuous DAC operation. The surface of inorganic tubular alumina membranes were modified to form the membrane contactors by using patterning to enhance contact surface area and employing a superhydrophobic agent coating to prevent solvent

slip and promote gas-only permeation. The performances of the developed membrane contactors were compared to more conventional polymer hollow fiber membrane contactors. The electrochemical regeneration cell (ERC) development included electrode and cell fabrications to facilitate and maximize hydroxide agent production at the cathode and CO_2 release at the anode. The ERC was explored with and without depolarization, first in batch mode using a half cell (<100 mL beaker-style cell) and an H-cell (< 100 mL inventory with cathode and anode compartments separated by a cation exchange membrane) under recirculating operation and then continuous operation. After the MC and ERC development, integration and performance testing was accomplished, including 24+ hours of performance operation to demonstrate initial stability and EH&S analysis. DAC performance validation on carbon management and energy requirement included in-situ and ex-situ measurements. The in-situ characterization methods included pH, voltage, current, CO_2, and O_2 measurements, while ex-situ characterization included inductively coupled plasma spectroscopy (ICP), carbon loading, and alkalinity measurements.

1.2 Key Results

This project's successful completion demonstrates that the UK CAER process, including hydroxide-based CO_2 capture from air coupled with electrochemical solvent regeneration, is an effective, robust, and flexible DAC process. The UK CAER-led team for this project included UK CAER and ALL4 Inc, with UK CAER developing the DAC process and ALL4 performing the environmental health and safety assessment (EH&S). ALL4 Inc independently concluded that the EH&S evaluation did not identify any unusual or significant environmental, health or safety concerns from the bench-scale studies. The process was not trading air emissions control for solvent contamination with severe environmental consequences. UK CAER's integrated process, including a modified inorganic membrane contactor and depolarized ERC for CO_2 capture and solvent conditioning, achieved >50% capture from air influent at > 2 L/hr while using < 3.5 V for solvent regeneration. The process generated H_2 as a co-product that can be sold, used for energy storage, or cost-saving depolarization of the DAC system during peak demand, and the process achieved an energy requirement of ~350 kJ/mol CO_2 with depolarization operated at < 1.8 V, compared to incumbent DAC technologies, where the energy intensive capture media can lead to energy requirements exceeding 373 kJ/mol CO_2. The testing and data collected from the 2 L/hr process provided a clear path for developing a TRL > 5 process through scale-up and validation at a > 10,000 L/hr scale process in the future. Summaries of activities from the key tasks are provided below.

Effectiveness of Micropatterned Superhydrophobic Membrane Absorber for DAC (Task 2):

UK CAER developed tubular membrane (inorganic) contactors with a larger internal diameter (ID) (3.5 mm) compared to commercial polymer membrane contactors with ~200 μm ID to reduce pressure drop across the membranes achieving <1 Pa/cm compared to the commercial membrane's 100 Pa/cm at a gas flow rate of 400 mL/min. A low gas-side pressure drop is important due to the large volumes of air that must be processed per mass of captured CO_2. The ceramic membranes were hydrophobized by fluoroalkyl silane (FAS) treatment to achieve contact angles > 120 degrees and liquid entry pressure > 50 psig. The contact angle was preserved for > 30 days in 2.5 wt% KOH. The membranes were micro-patterned to increase the contact area between influent CO_2 in the air and the capture fluid using micro sandblasting and laser etching approach. Micro

sandblasting achieved area enhancement of 25% but was limited by random roughness creation accompanied by destruction. The contact area was increased by more than 137% using laser etching, and the patterned membranes were used to form enhanced MCs by hydrophobizing their surface. The hydrophobized surface-enhanced membranes showed higher contact angles than the non-patterned membranes (140 vs. 130 degrees), likely due to the Cassie-Baxter/Wenzel effects (i.e., micro-features enhancing hydrophobicity) [1]. During testing with 5 wt% KOH as capture solvent and air influent at 20 mL/min (gas residence of 1.7 s), the area enhanced (137%) membrane achieved ~53% CO_2 capture compared to the unpatterned membrane that achieved 41% at similar conditions. The enhanced membrane was networked as a series of 4 membranes with a total geometric surface area of ~62 cm^2. The enhanced membrane achieved ~90% CO_2 capture from air (1.3E-06 mol/m^2-s, and residence time of 4.6 s) with 2 wt% KOH and performance similar to a polymeric membrane that achieved 96% capture (6.5E-07 mol/m^2-s, residence time of 0.8 s, surface area of ~132 cm^2).

Development of the Electrochemical Regenerator (Task 3):

UK CAER developed an electrochemical flow cell for solvent regeneration at low voltage, with initial material selection performed in beaker-style half-cells (electrodes in one chamber) and H-cells (a membrane separating the two electrodes in the cell) with the solution volume of < 100 mL. Cyclic voltammetry (scan voltage, while measuring current in forward and reverse direction to return to starting voltage) was performed in the half-cell with platinum (Pt), graphite, stainless steel 304, and Nickel-Copper (Monel™) evaluated as electrodes, and from testing, Nickel-Copper was chosen as the electrode for electrochemical flow cell construction due to its suitable anodic and cathodic performance. The H-cell was tested with/without hydrogen bubbling into the anode. Ni-Cu/Ni-Cu, Pt-based electrode/Ni-Cu, and Ti/Ti were tested as anodes/cathodes. The platinum-based electrode was integral to depolarization, suppressing > 1 V. For non-depolarized testing, the electrochemical flow cell was formed with a cation exchange membrane (Nafion), sandwiched by a flow space, which in turn is sandwiched by Monel electrodes and endplates with inlet-outlet ports. Parametric studies, including solvent flow rate (Q) at 5-50 mL/min, applied current (i) at 0-10A, and solvent concentration ($[K^+]$) of 5-15 wt% K_2CO_3, confirmed that as the loading factor, L_{K^+} ($= \frac{i}{[K^+]QF}$ i.e., current normalized by feed alkalinity, flowrate, and Faradays number) increased, the (i) pH decreased at the anode but increased at the cathode, (ii) alkalinity decreased at the anode but increased at the cathode, consistent with K^+ transfer from the anode to the cathode via the cation-selective membrane, and (iii) carbon loading remained relatively constant at the cathode but decreased at the anode consistent with the cathode generated hydroxide balancing K^+ transferred. The ERC produced near pH 14 solvent for use in the contactor for CO_2 capture and achieved a maximum CO_2 to O_2 ratio of 1.6. Gas-side measurement confirmed 100% charge efficiency for O_2 with CO_2 liberation at the anode controlled by pH. The depolarized ERC included a gas compartment next to the anode separated by a Porex membrane. The gas channel can be closed-off for non-depolarized operations. During ERC operation at 0.1 to 1 A, and depolarization achieved with externally supplied H_2 to the anode, O_2 evolution was suppressed, the operating voltage was reduced by ~1.4 V, and maximal H_2 utilization of ~50% was achieved.

Evaluation of EDEMS for DAC (Task 4):

UK CAER integrated an electrochemical regeneration cell and a membrane contactor to scrub CO_2 directly from the air and demonstrate their continuous operation. The integrated unit controlled the power supply and pump with input from the cathode pH in a feedback approach. Testing was

performed where the solvent was first conditioned by the ERC, followed by recirculation in the contactor shell for CO_2 capture, during which the regenerator remained off. For the ERC operated in the constant current mode at 0.5 A with H_2 externally supplied to the anode for depolarization, the nominal voltage was 1.1 V and effective charging required < 1 hour, resulting in ~315 J to boost the pH from ~12.2 to 12.6. (Non-depolarized operation required ~2.1 V). The enhanced membrane contactor with the cathode-produced solvent achieved 60% CO_2 capture from air influent at 2 L/hr (~5s residence time) and maintained the performance for 46 hours. During testing, ~9 x 10^{-4} moles of CO_2 were captured, leading to ~350 kJ/mol CO_2 energy requirement.

Process Report and Environmental, Health and Safety (EH&S) Assessment (Task 5):
ALL4 completed an Environmental Health and Safety (EH&S) assessment for UK CAER's lab scale integrated process for DAC. The assessment included a review of process flow diagrams, input and output flow rates for primary materials, literature describing similar processes and chemicals used or created during the process, actual air emission and wastewater test data and air emission calculations. The evaluation also included the identification of risks related to hazardous chemicals, air emissions, wastewater discharges, solid wastes generated and employee hazards. The assessment did not identify any obvious concern for the bench-scale operation and no apparent barriers to implementing the designed DAC system at a larger scale. Including H_2 generation, processing and storage for use as a fuel or source for fuel cell electrolysis at a commercial scale would involve more extensive safety precautions in equipment design, operation and storage facilities; however, these aspects are not unique and can be managed safely and efficiently following established and emerging standards. Additional testing at a larger scale was suggested to better quantify air emissions and potential waste issues derived from a commercial scale system. This project generated ~250 mL of spent capture solvent. This material was not identified as hazardous waste. A commercial facility may generate ~2,500 L (~660 gallons or twelve 55-gallon drums) of spent capture solvent that would not be routine and likely only be generated at decommissioning. UK CAER compiled a list of equipment, process, and performance data for a high-level design report for future DAC system design, techno-economic analysis, and life-cycle analysis. The design report included process flow diagrams, control systems layout, and major and auxiliary equipment.

2) BACKGROUND AND TECHNOLOGY DESCRIPTION

2.1 Project Background and Objective

This project developed and evaluated a novel electro-membrane system for the direct air capture of CO_2 toward mitigating the effects of a sustained increase in the atmospheric concentration of the greenhouse gas and its looming climatic implications. For DAC systems, the low concentration of CO_2 in the air, ~400 ppm, presents a significant challenge, requiring large energy input for recovery (thermodynamic minimum of 483 kJ/kg vs. 158 kJ/kg for DAC vs. post-combustion capture with 90% CO_2 recovery) while processing large volumes of air per fraction of CO_2 recovered leading to high-pressure drop and additional energy requirement. Currently, solvent and sorbent-based approaches are under consideration for DAC. Due to the low concentration of CO_2, strong interactions between CO_2 and a capture sorbent/solvent are required for effective removal, leading to high regeneration costs. Together, these facets make implementing a cost-effective DAC at scale (>1,000,000 tons per year) challenging. The UK CAER technology employs a low-

temperature coupled electrochemical-membrane capture and regeneration technology that simultaneously captures and up-concentrates ambient CO_2 while regenerating the capture media. Concurrently, the technology also generates H_2 as a byproduct that can be sold, used for energy storage or cost-saving depolarization and deoxygenation of the DAC system. H_2 production provides a commercial appeal, unlike other DAC systems' limitation to CO_2 as the only product without further processing steps.

The UK CAER DAC process is a solvent-mediated process where the use of KOH as the capture solvent presents several benefits, including chemical stability, recyclability, fast kinetics for CO_2 capture, and near "zero" ppm dissolved CO_2 to maximize the driving force for CO_2 absorption, and the compatibility for cathodic (negative electrode) electrolytic regeneration at low voltages.

The specific objectives of the project were to (1) develop a ceramic membrane contactor absorber including a patterned surface and demonstrate its effectiveness for ambient CO_2 removal, (2) demonstrate stable absorber performance and contrast to a traditional polymer membrane contactor, (3) develop and demonstrate the effectiveness of a depolarized ERC for the respective regeneration and concentration of both the capture solvent and CO_2 at low applied voltages, (4) demonstrate stable performance for the electrochemical regeneration process, and (5) integrate and demonstrate the enhanced depolarized electro-membrane system (EDEMS) for 50% CO_2 capture from a > 2 L/hour influent air with ~400 ppm CO_2.

All Project Success Criteria were satisfied and are shown in **Exhibit 2.1.1**

Exhibit 2.1.1 Success Criteria for DE-FE0031962.

	Success Criteria	**Performance Achieved**
1	Production of a patterned membrane contactor with an improved membrane area of 10-25% compared to the non-patterned membrane.	Achieved 24.4% membrane area enhancement via micro-blasting with 17.5 µm aluminum oxide abrasive for 15 s and achieved 137% enhancement via laser etching.
2	Membrane contactor achieves 50% CO_2 capture efficiency	Achieved ~53% CO_2 capture from air with patterned inorganic membrane contactor with a 1.7 s gas residence time in the contactor and 5wt% KOH as capture solvent. Achieved ~90% CO_2 capture from air with patterned membrane contactor module with a 4.6 s gas residence time in the contactor and 2 wt% KOH as capture solvent with performance maintained for ~ 20 hours.
3	DEC achieves > 50% faradaic efficiency at 1 A	DEC suppressed voltage requirement by ~1.4 V via anode depolarization at 1 A. O_2 faradaic efficiency for the non-depolarized process was ~100%. The H_2 utilization for depolarization is estimated at ~50%.

4	EDEMS achieves > 50% CO_2 capture efficiency at < 3.5 V DEC and < 10 psig	A depolarized integrated system operating at 0.5A and < 1.2 V achieved ~60% CO_2 capture efficiency from 2 L/hr influent air (~5 s residence time), including a stable performance for over 80+ hours where the capture performance depended on the pH swing from 12.2 to 12.6. Pressure drop was < 0.005 psig

The knowledge gained from the execution of DE-FE0031962 includes the following:

1. *The loading factor is integral to the electrochemically-enabled carbon absorption, concentration, and release process.* The UK CAER process provides basification and acidification to accompany carbon capture and release in concentrated form by electrolysis. The loading factor as a lumped parameter, i.e., current normalized by feed alkalinity and flow rate, was found to control the extent of pH swing, such that high loading factors lower the pH at the anode and increase the pH at the cathode. Furthermore, the loading factor affected the K^+ transport efficiency, where loading factors >1 exacerbate proton crossover and consequently reduce pH swing.
2. *Anode depolarization stabilizes the anodes.* During stress-testing of the ERC at high currents, the resulting voltages can be high, leading to anode corrosion from large overpotentials, e.g., carbon corrosion via $C + H_2O \leftrightarrow C\text{-}O_{ads} + 2H^+ + 2e^-$ when configured as a part of the anode. However, during anode depolarization with H_2, in addition to suppressing reactions that lead to O_2 evolution, depolarization also suppresses other anode reactions.
3. *Implementing an alternate reactor design can maximize carbon dioxide.* The electrochemical reactor design implemented during this project can achieve a high CO_2 to O_2 ratio. However, by leveraging knowledge from electrochemical reactor design, a complete separation of the species can be achieved, thereby avoiding the need for any downstream purification but at the cost of slightly increased voltage.
4. *Optimization of bubble dynamics is important to minimizing voltage loss and energy consumption.* During typical operation of the ERC, H_2 and O_2 gases evolve at their respective electrodes. However, the rapid evolution of gas into the flow space can separate the working fluid/electrolyte from the electrode leading to large resistance and voltage inefficiencies. A sufficient flow rate ameliorated the impact of gas bubbles but can affect the loading factor requirements for operation. A key aspect of post-project work is exploring surface tension optimization for fast bubble detachment.
5. *Flouro-alkyl silane (FAS) on the ceramic membrane is very stable in a basic environment.* The UK CAER capture process requires a basic environment for fast capture from low concentration CO_2 feed. The caustic nature of the solvent can be challenging for polymeric materials. FAS was stable during long-term testing and conducive to forming a contactor due to its resistance to chemical attacks.

2.2 Process Description

Unlike capture from point sources, the low concentration of CO_2 in the air presents a significant challenge **(Exhibit 2.2.1)**. For example, compared to coal capture with 14 vol% CO_2, air possesses 0.04 vol%, a 600 times reduction in concentration and driving force. As a result, strong interactions are required between the dilute CO_2 and the binding media for capture, leading to costly regeneration cycles.

The UK CAER process employs OH^- mitigated facile capture from the air and is a near-closed-loop process on the solvent side and involves using only two major unit operations, including an electrochemical regenerator cell (ERC) and membrane contactor (MC). Unlike typical solvent-based air capture processes requiring elevated temperatures (thermal-swing) for solvent regeneration, it operates under ambient conditions. CO_2 from air is captured in the contactor with an alkali-metal OH^--based solvent, and this solvent is regenerated at the ERC's cathode (negatively-biased electrode), simultaneously with CO_2 up-concentration and release for storage or utilization at the anode (positively-biased electrode). A schematic of the UK DAC process is shown in **Exhibit 2.2.2**.

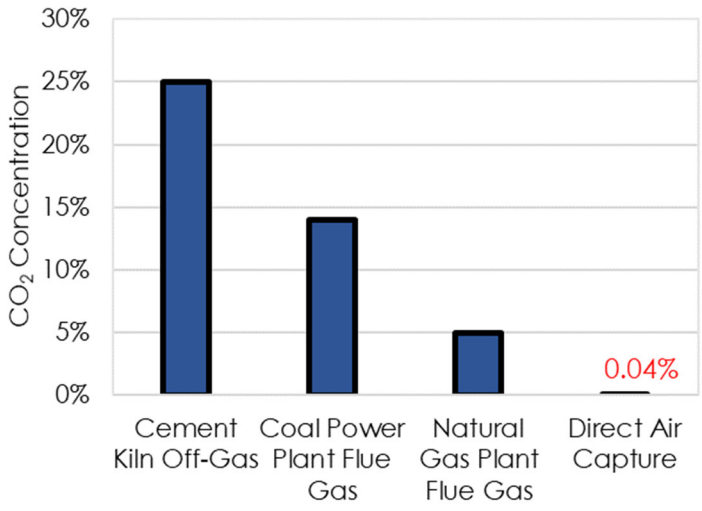

Exhibit 2.2.1. CO_2 concentration from different sources.

The MC features α-alumina type ceramic membranes with superhydrophobic and expanded surfaces where influent ambient CO_2 is absorbed into the capture solvent via the membrane with the equilibrium CO_2 partial pressure difference between 400 ppm CO_2 in the air (40 Pa) and dissolved CO_2 (~0 Pa for KOH), providing the driving force, and reaction with KOH via $CO_{2\,(dissolved)} + 2KOH \leftrightarrow K_2CO_3 + H_2O$ ($CO_2 + K_2CO_3 + H_2O \leftrightarrow 2KHCO_3$ is not facile due to low CO_2 concentration in the air) providing capture and maintaining the driving force. The rate of CO_2 absorption can be estimated, $R_{CO2} \approx C_{CO2} K_H \sqrt{D_{CO2} k C_{OH}}$ where C_{CO2}, K_H, D_{CO2}, k (~10 $m^3 mol^{-1} s^{-1}$), and C_{OH} are the CO_2 concentration in air, henry's constant, the diffusivity of CO_2, rate constant, and concentration of HO^-, and it follows that reduced and low OH^- concentration resulting from capture leads to diminished capture rate. Counter-current operation is also employed to preserve the driving force. Following capture, $K_2CO_3/KHCO_3$ from the membrane exits to the ERC to liberate CO_2 in concentrated form. In the ERC, water splitting reactions including the H_2 evolution reaction (HER, $2H_2O$ + electrons = $H_2 + 2OH^-$) and O_2 evolution reaction (OER, $2H_2O = O_2 + 4H^+$ + electrons) control pH.

To reduce energy cost, the ERC leverages depolarization by using H_2 (from HER at the cathode or supplied externally) for the H_2 oxidation reaction (HOR, $H_2 = 2H^+ +$ electrons) in place of the oxygen evolution reaction (OER) at the anode. When H_2 depolarizes the anode, the minimum theoretical voltage (excluding all polarization losses) reduces to 0 V vs. 1.23 V for the non-depolarized scenario. The $K_2CO_3/KHCO_3$ from the contactor is fed to the anode side, where K^+ ions in solution are attracted to the negatively charged cathode and are transported via a cation exchange membrane (e.g., Nafion or Neosepta CMX) to the cathode to combine with OH^- (recreating the capture solvent), while CO_3^{2-} or HCO_3^- is converted to CO_2 in sequence by reacting with protons produced at the anode via $CO_3^{2-} + H^+ = HCO_3^-$ followed by $HCO_3^- + H^+ = CO_2 + H_2O$. In the UK CAER process, the concentration of the K^+-based solvent is adjustable with internal recirculation.

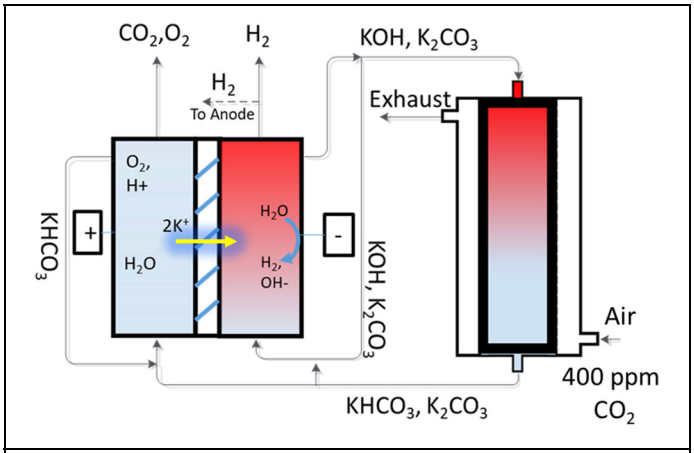

Exhibit 2.2.2. Schematic of UK CAER setup used to capture CO_2 from air. Pictures of the electrochemical regeneration cell (b) and membrane contactor (c).

The UK CAER process operated at 22-25°C, with initial performance demonstrated in the separate units of the MA and ERC before integration. During performance evaluation, pH, flow rate, alkalinity, concentrations, pressure, contact angle, power, voltage, and current were used to assess effectiveness. Details of the process development for the MA and ERC are discussed in **Section 3,** along with their results. After process integration, 40+ hours of testing were conducted for the EH&S assessment.

3) PROJECT TECHNICAL RESULTS

3.1 Developing an Effective Membrane Absorber for DAC

<u>Patterning of Ceramic Membranes for Forming Membrane Contactors</u>

UK CAER began the project by fabricating 3.5 mm internal diameter (ID) porous ceramic membrane contactors with enhanced specific surface area to enable low-pressure drop operation and effective capture of CO_2 from air. Tubular porous alumina was explored as a substrate for preparing the inorganic membrane contactor, and two methods were investigated for patterning this substrate, including a micro-blasting (AccuFlo and ProCenter System at COMCO Inc.) and laser etching (50-watt CO_2 Universal Laser Systems VLS3.50). The alumina substrate was 87 mm long and had an OD of 5.7 mm. For demonstrating microblasting, the tubes were treated with 10, 17.5, 50, and 89 µm aluminum abrasives. The treatment time for each tube was ~15 seconds, and their surfaces were characterized using a Zygo optical profilometer. **Exhibit 3.1.1 (a-c)** shows the surface roughness profiles of a pristine and 17 µm abrasive and 89 µm abrasive micro-blasted membrane. A roughened surface was observed for the pristine membrane and further restructuring

for the micro-blasted membranes. In comparison to the pristine membrane, the micro-blasted membranes show the larger hill to valley profiles, as expected. **Exhibit 3.1.2** summarizes the treatment results for the membranes treated with different-sized alumina oxide. SDR is the developed interfacial ratio, which is the increase in the surface area created through the texturing process compared to a geometrically smooth surface. Compared to the un-treated tube, the 17.5µm blasted membrane had the largest SDR increase from 90% without treatment to 112%, which is about a 24% increase in the surface area. However, considering the randomness of the restructuring whereby surface area creation can be accompanied by destruction, this approach had limited applicability.

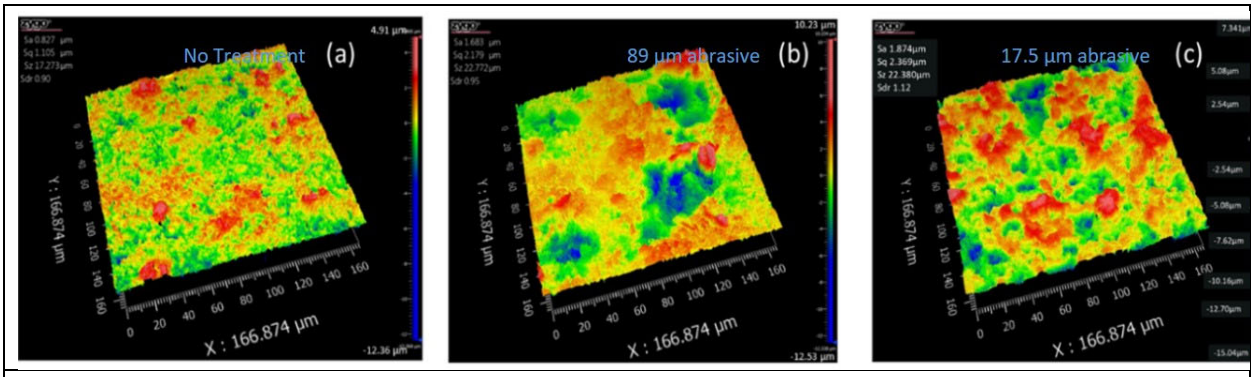

Exhibit 3.1 1. Optical profilometer of pristine (a), 89 µm abrasive (b), and 17 µm abrasive (c) micro-blasted membrane.

Exhibit 3.1.2. Surface characteristics of micro-blasted membranes.

Abrasive, Aluminum Oxide (µm)	10.0	17.5	50.0	89.0	No Treatment
SDR, Developed interfacial area ratio (%) *vs.* geometrically smooth surface	90.0	112.0	88.0	95.0	90.0
Area Enhancement (%)	None	24.4	None	5.6	None

Laser patterning was explored as an alternative method to the microblasting approach to provide patterning flexibility, as laser engraving can facilitate the introduction of different micropatterns on the membrane surface to enhance membrane performance. During laser patterning, the solid material was removed from the material surface when bombarded by a laser beam with sufficiently high power density. **Exhibit 3.1.3** (**a-f**) shows the optical images of laser engraved alumina tubes with various patterns and conditions. **Exhibit 3.1.3 (a)** is a line pattern with a space of 200 µm. The resolution of the laser spot was ~ 200 µm, including its melting area, implying that as the laser moved along the membrane surface to excavate materials, when neighboring lines were too close to each other, it was difficult to distinguish the line patterns. Interestingly, such a line pattern allows fast laser carving because of the minimum turns and stops, and assuming a bunch of alumina tubes could be laid side by side, then this line pattern might need about 22 hours per pass to treat a 1 m^2 surface area of the alumina tubes with a 50-wattage laser engraver at 30% speed. The duration would decrease if a more powerful machine were used, e.g., a 200-wattage machine. **Exhibit 3.1.3 (b)** is a staggered line pattern with a space of 360 µm between lines, and a clear staggered line profile is observed in the digital image.

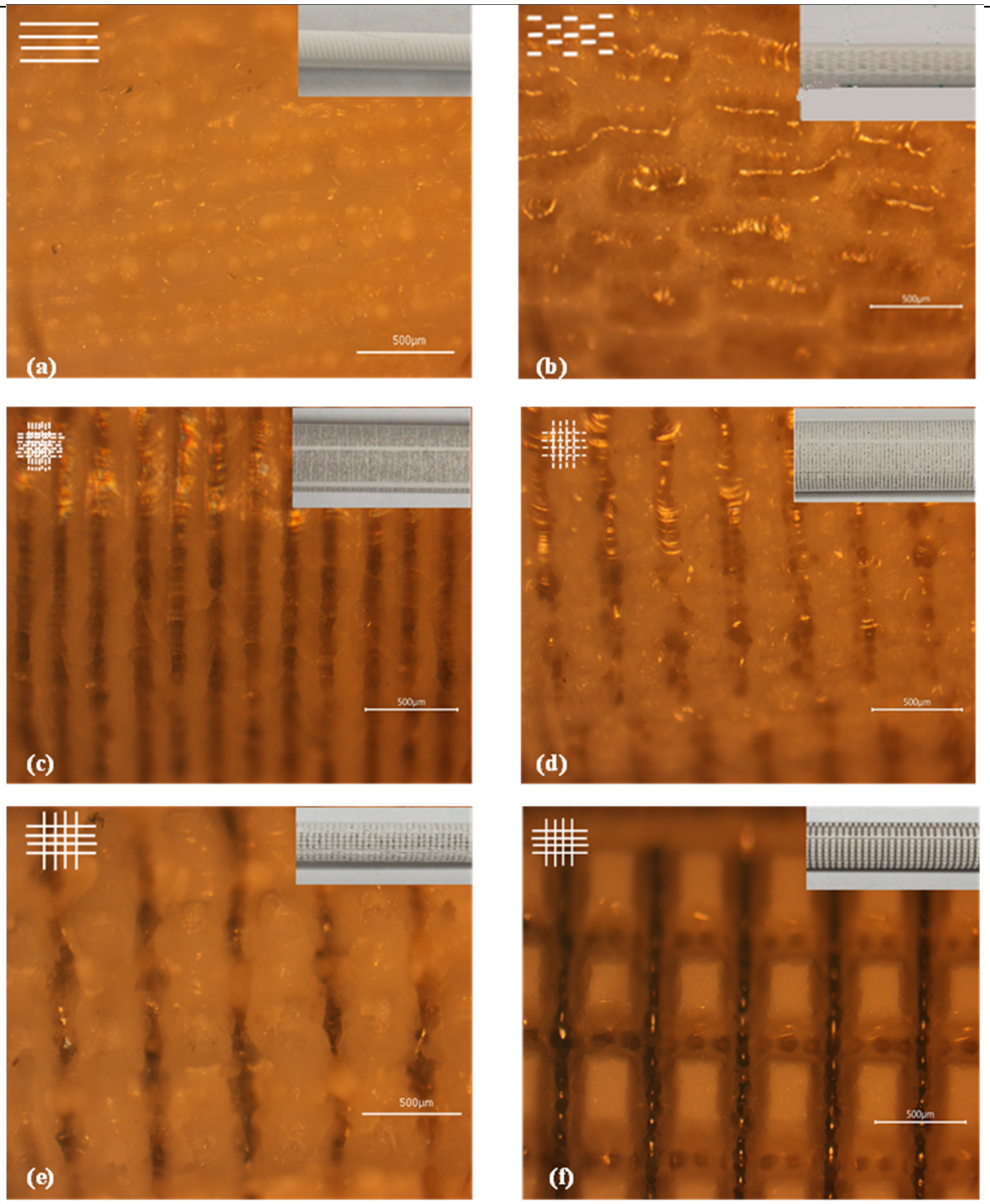

Exhibit 3.1.3 Digital images for different laser carving patterns (shown on the top left corners) on the outer surface of alumina tubes, (a) Longitudinal line pattern with a space of 200 µm under water, 4 passes (b) Staggered longitudinal line pattern with a space of 360 µm under water, 2 passes (c) Dash grid pattern with a space of 200 µm under water, 1 pass (d) Dash grid pattern with a space of 360 µm under water, 2 passes (e) Solid grid pattern with a space of 500 µm under water, 6 passes and (f) Solid grid pattern with a space of 500 µm in air, 5 passes.

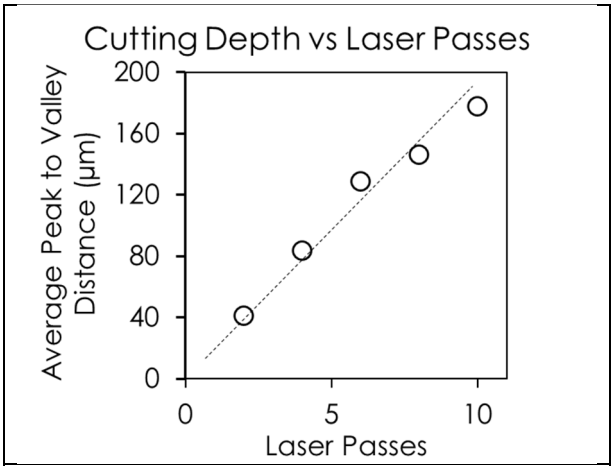

Exhibit 3.1.4. Effect of Laser Pass on Etch Depth.

Exhibit 3.1.3 (c) and **(d)** are dash line grid patterns with a space of 200 µm and 360 µm with a lower pass (one pass and two passes, respectively). These demonstrate that finer microfeatures were formed by tuning the patterns, e.g., with the dashed line grid pattern, features close to 200 µm are formed. However, the patterns become smeared with more passes due to the limitation of the laser engraver. In addition to performing laser engraving with a wet membrane, **Exhibit 3.1.3 (e)** and **(f)** show the grid patterns with a spacing of 500 µm with the laser carving performed under water and in air. For the pillar structures formed in the air, their boundaries were sharper without the interference from water. These grid patterns require ~25 hours per pass to treat ~1 m^2 surface area of the alumina tubes. From **Exhibits 3.1.2 (a-f)**, laser engraving provides flexibility for patterning ceramic alumina membranes. Furthermore, such patterning can have implications for mass transfer. For example, staggered line profiles similar to **Exhibit 3.1.3(b)** have been reported for porous polyvinylidene fluoride (PVDF) membrane contactors to increase the gas flux across the membrane by 20-30% due to the microgrooves forming low shear gas-liquid interfaces, resulting in the local slip at the gas-liquid interface [2]. Furthermore, the cutting depth of the laser was found to linearly depend on the number of laser passes (**Exhibit 3.1.4**), allowing for creating a larger membrane contact area.

In order to more accurately estimate the outer surface area increase from the laser micropatterns, Micro CT was employed. The scanning was performed with a voxel size of 2.4 µm and a total length of 6.0 mm. **Exhibit 3.1.5** shows the 3D model generated from the CT scanning. The outer surface area for the 200 µm line pattern (4 passes) increased by 79% compared to the unpatterned membrane, while the surface area for a 500 µm solid grid pattern (6 passes) increased by 137% compared to the un-patterned one, which is close to the theoretical value of 96% assuming 500 µm pillar structures. The differences could be from the finer microstructures shown in the SEM image (**Exhibit 3.1.5**). Due to the 2.4 µm voxel size, the model of the un-patterned membrane shows a smooth surface, and its outer surface area from the 3D model matches the calculated value from its geometry value with only a 2% difference. Due to the interaction between the water and the air, the surface morphology of the line patterned membrane has a wave-like structure, as shown in the SEM image in **Exhibit 3.1.5 (a)**. The porous structures are possible from the interaction between the alumina melt and water sprouting from under the porous tube. As shown in the embedded SEM in **Exhibit 3.1.5 (a)**, the inner pore surface forms an interesting structure, possibly from the interaction between the alumina melt and water. The grains became tighter, and the gaps among these grains were close to 100 nm. The SEM in **Exhibit 3.1.5 (b)** clearly shows the laser-treated area, i.e., the melt area, and the pillar area without the melt. **Exhibit 3.1.4 (c)** shows that the un-patterned surface also has some microfeatures formed by the alumina grains. The detailed surface area values for three tube-set are listed in **Exhibit 3.1.6**. In summary, from exploring microblasting and laser blasting for membrane patterning, 24.4% membrane area enhancement was achieved via micro-blasting with 17.5 µm aluminum oxide abrasive for 15 s, whereas using laser etching to

carve line patterns onto the alumina membrane, an estimated 137% area enhancement was obtained. Furthermore, the laser approach demonstrated more flexibility for patterning the ceramic membrane.

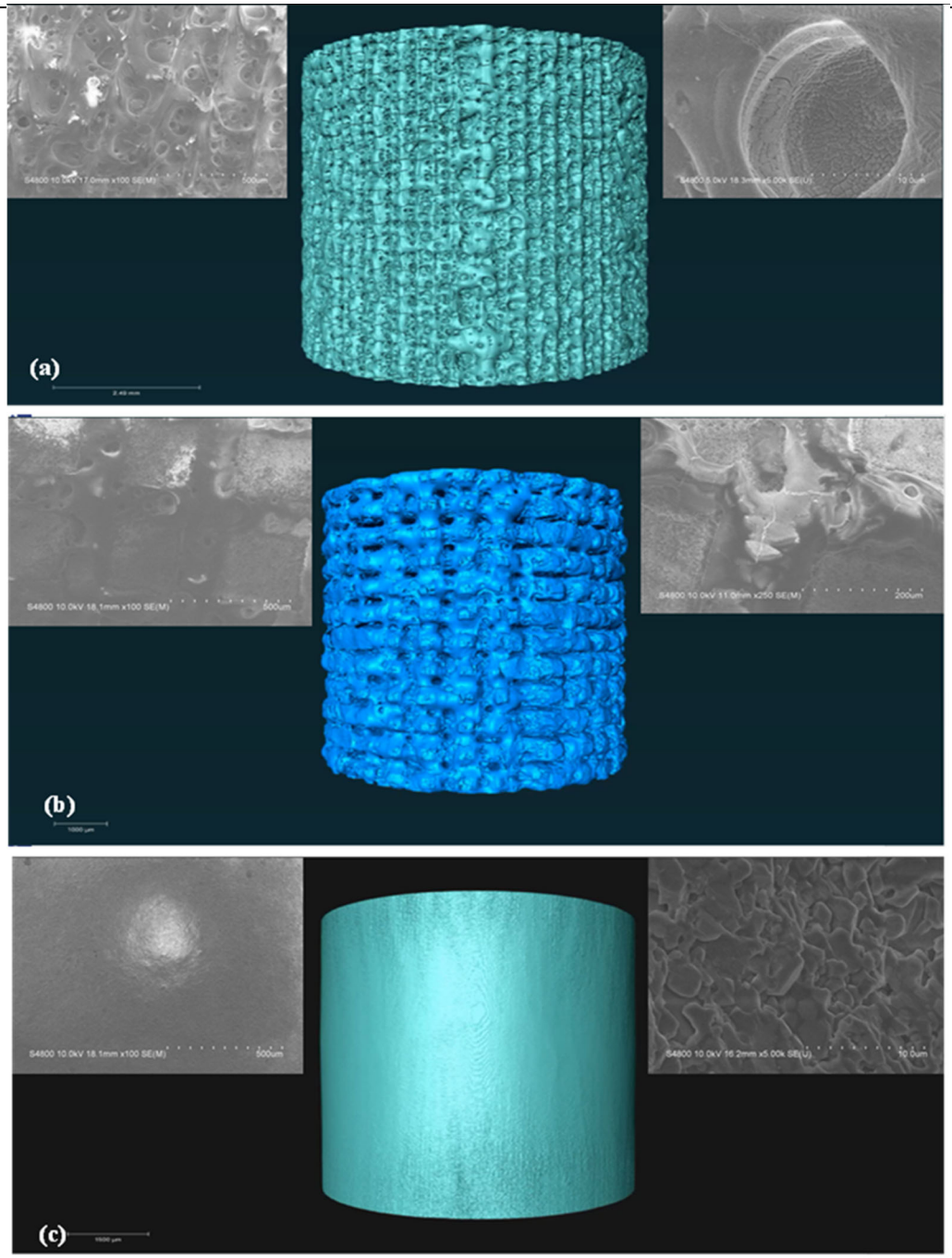

Exhibit 3.1.5. 3D Model from Micro CT (center) and corresponding SEM images with various magnifications (top left and right) of (a) Longitudinal line pattern with a space of 200 µm under water, 4 passes (b) Solid grid pattern with a space of 500 µm under water, 6 passes and (c) Un-patterned samples.

Exhibit 3.1.6. Characteristics of Laser Patterned Membranes

Tubular Alumina Membranes	Un-patterned	200 µm Line Pattern	500 µm Grid Pattern
Surface Area from Micro CT (cm^2)	62.8	112.4	148.8
Surface Area Increased percentage from Micro CT (%)	2	79	137

Superhydrophobic Modification of Micropatterned Membrane Contactor

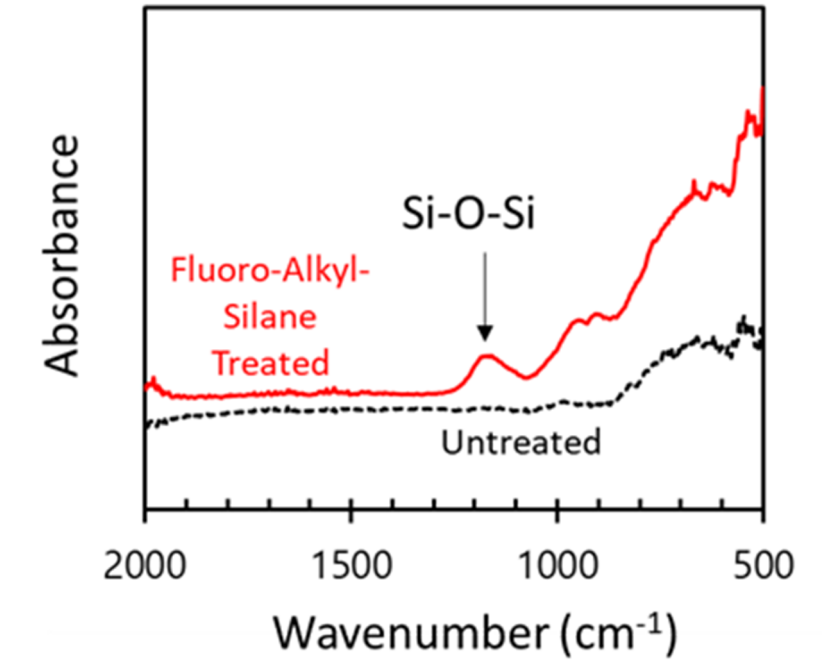

Exhibit 3.1.7. FTIR/ATR scans for the untreated and FAS-treated membranes.

After developing the methodologies for membrane patterning, the membrane contact face required hydrophobization to function as an MC. For initial MC development, generally, the pristine alumina membranes were treated with fluoroalklysilane (FAS) to introduce hydrophobicity. The membrane was washed with acetone, deionized (DI) water, and then dried. After drying in an oven at 60 ºC for 1 hr, the tube was immersed in 0.1 M NaOH solution and kept in the oven at 80 ºC overnight. Afterward, the tube was immersed in DI water overnight and dried in an oven at 60 ºC. The tube was put into a PTFE vial with 50mL 0.02M FAS/*n*-hexane solution, and the vial was then immersed in a 40 ºC water bath and sonicated for 4 hours and then overnight for 20 hours. Finally, the tubes were soaked with *n*-hexane overnight. The process was repeated one more time to add more layers. FTIR/ATR spectra of the untreated and FAS-treated membrane (**Exhibit 3.1.7)** confirm the presence of Si-O-Si vibrations consistent with the FAS treatment.

The water contact angles of the unpatterned and laser-patterned alumina membranes were measured after the FAS treatment. The contact angle without FAS treatment could not be measured because the water droplet quickly got sucked into the porous membrane. As shown in **Exhibit 3.1.8** and summarized in **Exhibit 3.1.9**, after grafting with FAS, the membranes showed various contact angles in response to the laser carving patterns.

Exhibit 3.1.8. (a)-(b) show a typical snapshot during the contact angle measurement performed with a Biolin Scientific optical tensiometer. The hydrophobicity of the patterned tubes, except the staggered line pattern, increased compared to the un-patterned, thus indicating that the pattern with micro features could result in the Cassie–Baxter wetting state. The decreased contact angle from the staggered line pattern could be from large features due to the smaller number of passes and the reduced density of the patterns. While for the patterns with 200 µm space, i.e., either longitudinal line or dash grid, the contact angle increased regardless of the number of passes. This indicates that the patterns' coverage over the tubes' outer surface, including changes due to the melting and reforming from the laser ablation, may play a key role instead of the number of passes, i.e., the depth, on the contact angle. This is further revealed when comparing the 500 µm solid grid patterns with 6 passes with the 360 µm dash grid patterns with 2 passes. Despite the smaller number of passes, the contact angle of the 360 µm dash grid patterns is still greater. Compared with the water submerged laser-engraved tube, the contact angle of the 500 µm solid grid pattern in air indicates a very minimal effect of the laser bath medium on the contact angle.

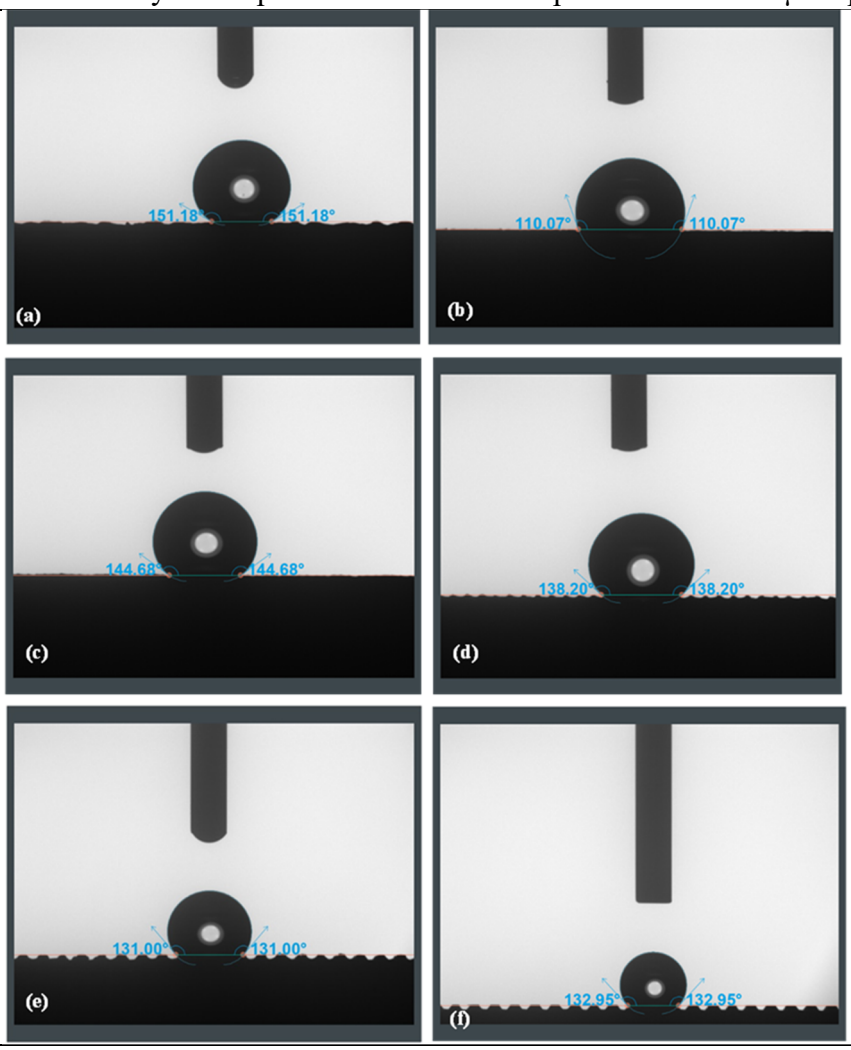

Exhibit 3.1.8. Snapshots perpendicular to the longitude on the outer surface of alumina tubes with different laser carving patterns (a) Longitudinal line pattern with a space of 200 µm under water, 4 passes (b) Staggered longitudinal line pattern with a space of 360 µm under water, 2 passes (c) Dash grid pattern with a space of 200 µm under water, 1 pass (d) Dash grid pattern with a space of 360 µm under water, 2 passes (e) Solid grid pattern with a space of 500 µm under water, 6 passes and (f) Solid grid pattern with a space of 500 µm in air, 5 passes.

Exhibit 3.1.9. The contact angle of various alumina membranes with FAS treatment.

Pattern	Space (µm)	Pass Cycles	Laser Carving in Water or Air	Contact Angle (°)
Longitudinal Line	200	4	Water	146
Staggered longitudinal line	360	2		113
Dash grid (both longitudinal and circumferential dash lines)	200	1		145
Dash grid (both longitudinal and circumferential dash lines)	360	2		138
Solid grid (both longitudinal and circumferential solid lines)	500	6		135
Solid grid (both longitudinal and circumferential solid lines)	500	5	Air	132
Un-patterned	N/A	N/A	N/A	127

In order to further demonstrate the FAS-treated ceramic membranes as MCs in a hydroxide-mediated capture system, their stability was evaluated by soaking in 2.5% KOH, where FAS dissolution precedes membrane wetting and increase in mass transfer resistance. **Exhibit 3.1.10** shows the contact angle measurement for FAS-Treated MC (200 µm line patterned, 4 passes) in 2.5wt% KOH solution, along with contact angle changes after extended exposure to KOH. Polypropylene (PP) membranes with pore sizes of 0.2 and 0.45 µm were purchased from Sterlitech and tested for comparison since they form the backbone for commercial polymeric membrane contactors. **Exhibit 3.1.10** shows that the contact angle was stable for FAS MC, showing ~94% relative stability after 120 hours and >85% relative stability after a cumulative 12 days in 2.5 wt% KOH. After almost 5 weeks, the FAS MC retained almost 80% of its starting contact angle, similar to the polypropylene membranes.

Exhibit 3.1.10. Contact angle preservation with soaking in 2.5wt% KOH at room temperature

Membrane	Contact Angle (°)	Contact Angle after 72hours in 2.5wt% KOH at ~23°C (°)	Contact Angle after 120hours in 2.5wt% KOH at ~23°C (°)	Contact Angle after 12 days in 2.5wt% KOH at ~23°C (°)	Contact Angle after additional three weeks in 2.5wt% KOH at ~23°C (°)
FAS Membrane Contactor	131	123	123	113	104
PP membrane, 0.2 µm	135		127		120
PP membrane, 0.45 µm	132		126		115

Performance of Membrane Contactors for DAC Applications

UK CAER assembled a lab-scale CO_2 capture apparatus (**Exhibit 3.1.11**) to evaluate the membrane absorber, including a mass flow controller for gas control, a liquid pump for circulating the capture solvent, gas analyzers, and pH loggers. Acid and water traps are installed at the exit of

the contactor to mitigate capture measurement error from solvent crossover and protect the CO_2 sensing equipment downstream.

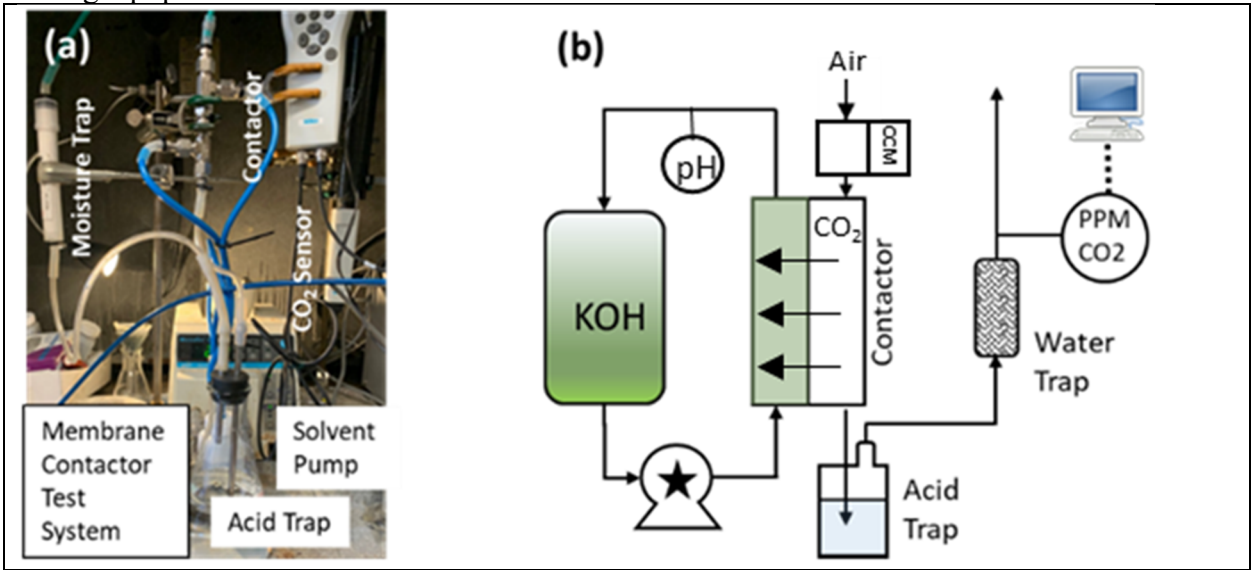

Exhibit 3.1.11. Pictures (a) and circulating batch-mode schematic (b) of the membrane contactor experimental setup.

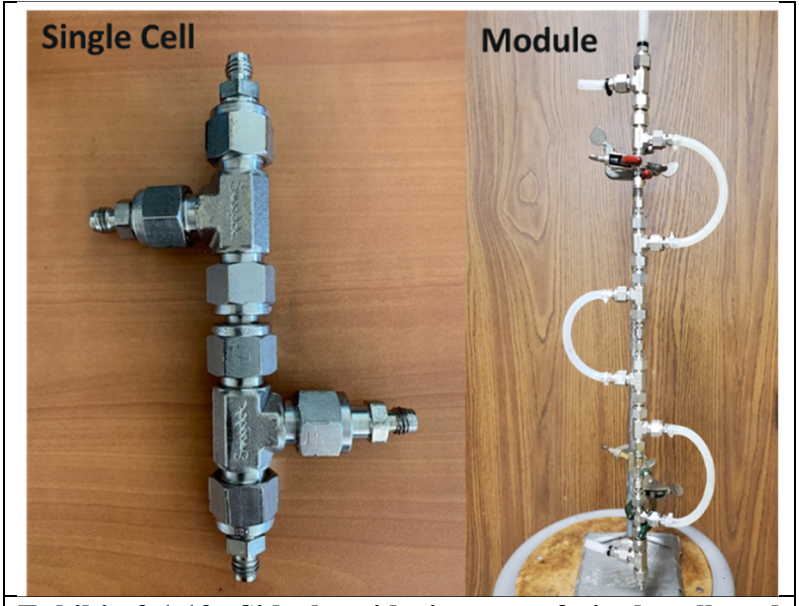

Exhibit 3.1.12. Side by side images of single-cell and serial module membrane contactors.

Non-patterned and patterned inorganic tubular membranes with FAS coating were assembled into modules composed of four single cells in series (**Exhibit 3.1.12**) and were tested as the contactor in a circulating batch mode operation with 2-5% KOH at 50 mL/min on the shell-side as capture solvent and single-pass CO_2 from air influent at ~30 mL/min on the lumen side of the membrane. The membranes in the single-cell had a length of 87 mm, an outer diameter of 5.7 mm and an inner diameter of 3.5 mm. The membrane module had a superficial membrane area of 62.8 cm^2.

The single cells used to form the patterned membrane bundle comprised membranes with grid patterns spaced 500 µm apart. During laser etching, 50% laser power (~33W) was employed with 5 passes underwater on the alumina tube with a nominal pore size of 0.5 µm. **Exhibit 3.1.13.** shows that the patterned membrane achieved ~90% capture with 2% KOH as capture solvent and air influent at 30 mL/min (gas residence of 4.6 s) in comparison to the unpatterned membrane that achieved ~66% at similar conditions. The capture performance was similar to a polymeric

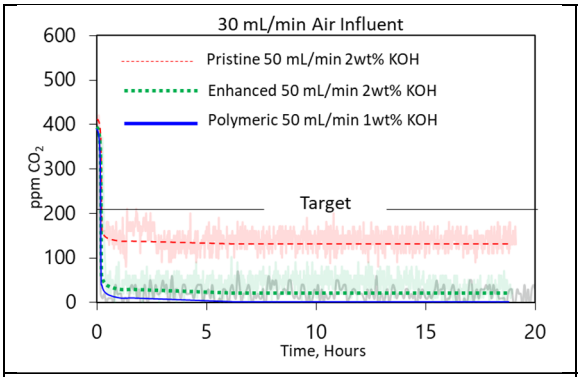

Exhibit 3.1.13. CO_2-direct air capture performance with non-patterned alumina and patterned alumina contactors with ~ 400 ppm CO_2 in air influent at 30 mL/min and 50 mL/min 2wt% KOH as capture solvent. Performance compared to Commercial polymeric contactor.

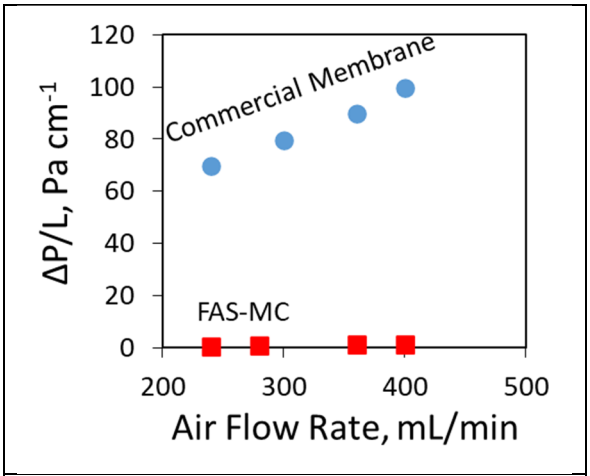

Exhibit 3.1.14. Air pressure drop per unit tube length for the UK CAER MC compared to a commercial membrane contactor.

membrane which achieved ~96% capture (tau 0. 8 s, surface area ~132 cm^2).

However, as shown in **Exhibit 3.1.14**, the pressure drop requirements significantly differ by over 50X, owing to the large tubular ID of 3.5mm for UK CAER FAS MC compared to <300 µm ID tubes used to form the polymeric MC leading to their increased pressure drop. **Exhibit 3.1.15** contrasts the performance of the non-patterned and patterned single membranes to their four serial membrane module format and shows that patterning and/or increases in residence time (and surface area) and solvent concentration improved capture efficiency. Summarily, increasing residence time increased capture efficiency but not flux (comparing single non-patterned and patterned membranes, 1.1 s vs. 1.7 s residence time), increasing capture solvent concentration increased both capture efficiency and flux (comparing module non-patterned membranes 2wt% vs. 5wt %), and patterning increased both capture efficiency and flux (comparing single and bundle membranes at similar conditions). In addition, comparing the non-patterned single cell and module at a similar concentration and flow rate (30 mL/min) shows a flux decrease from 3.9 x 10^{-6} mol/m^2-s to 2.9 x 10^{-6} mol/m^2-s which suggests driving force reduction along the serial membrane bundle.

Exhibit 3.1.16. shows the result from long-term DAC operation with the four serial 500 µm grid-patterned membranes at the air flow rate of 30 ml/min inside the lumen side of the membrane contactor and an alkaline solution on the shell side. The total testing comprised three stages and lasted for 220 hours. The pH of the absorbent at the first stage was maintained above pH 13-14 with a continuous pH adjustment. The first stage lasted 138 hours, and the average carbon dioxide removal efficiency was about 96%. For the second stage, the membranes were washed with DI water and dried at 80 °C overnight. The membrane kept the same LEP of 3.5 bars, as shown in **Exhibit 3.1.16.** The liquid entry pressure (LEP) of the membrane contactor was measured by passing DI water on the shell-side of the membrane and gradually pressurizing until the first liquid droplet was observed on the tube side. The LEP indicated the wetting resistance of the membrane.

Exhibit 3.1.15. Performance characteristic of non-patterned and patterned alumina contactors direct air capture of CO_2.

No . Membranes #	Fabrication	Geometric Area m²	K_2CO_3 %	Capture %	Residence Time s	Flux mol/[m²-s]
1	Pristine	0.000793	5	30%	1.1	3.9E-06
1	Pristine	0.000793	5	41%	1.7	3.6E-06
1	Patterned	0.000793	5	46%	1.1	5.9E-06
1	Patterned	0.000793	5	52%	1.7	4.5E-06
4	Pristine	0.00317	2	66%	4.6	2.1E-06
4	Pristine	0.00317	5	90%	4.6	2.9E-06
4	Patterned	0.00317	2	90%	4.6	2.9E-06

The membranes were reassembled and evaluated with a 2 wt% KOH without any pH control. Within 72 hours, the solution pH dropped from pH 12.8 to pH 12.5 with the CO_2 absorption. The average capture efficiency was around 95%. Due to the drop in pH, the removal efficiency at the end of the second stage dropped down to 71%. Therefore, in the third stage, a newly prepared 2 wt% KOH solution was refreshed into the system, and the removal efficiency recovered to 95%. After the test, the membranes were washed and dried at 80 °C. The LEP was tested again and was stabilized at 3.5 bars. The results from **Exhibit 3.1.16 and Exhibit 3.1.17** confirmed that the periodic drying method could be feasible to refresh the alumina membrane contactor, presenting an additional benefit over the commercial polymeric MCs. Furthermore, the integration of the MC with a pH control source as the ERC will facilitate stable operation, as demonstrated in stage 1.

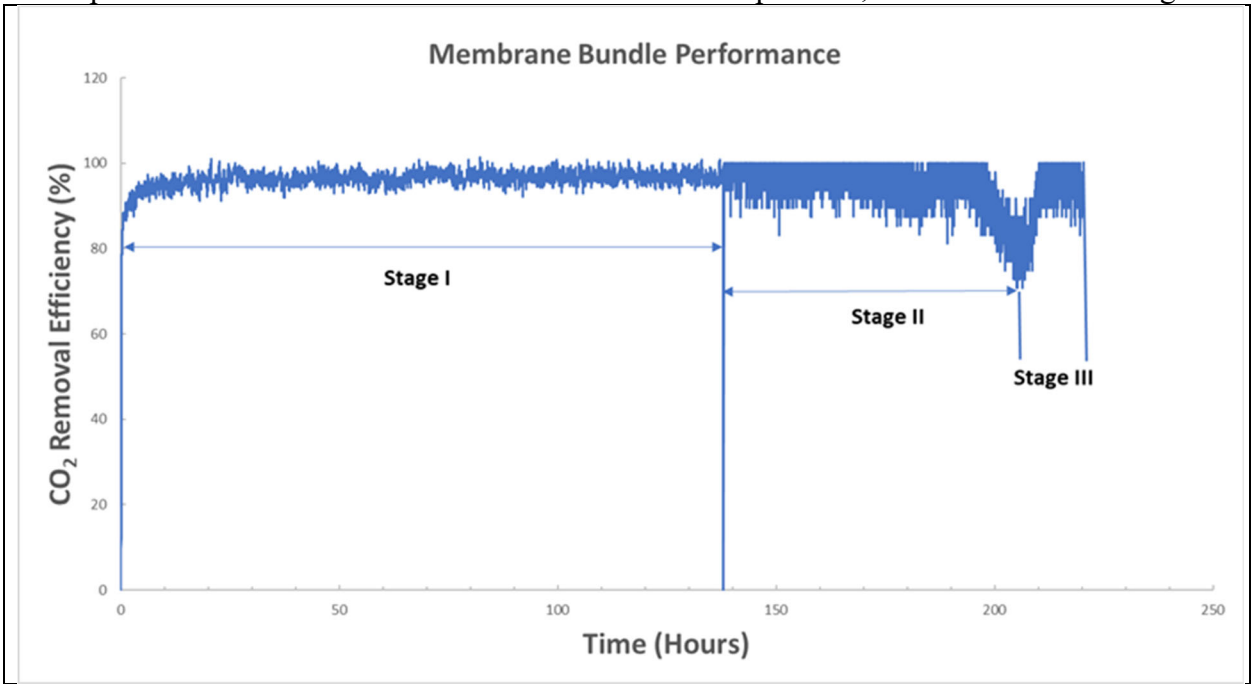

Exhibit 3.1.16. Effect of various operation conditions on CO_2 removal efficiency of four serial 500 µm patterned alumina membrane bundles with the airflow rate of 30 ml/min (Stage I: absorbent of 10 wt% K_2CO_3/KOH at a flow rate of 25 ml/min with pH control at 13 to 14; Stage II: absorbent of 2 wt% KOH aqueous solution at a flow rate of 50ml/min without pH control; Stage III: Refresh with new absorbent of 2 wt% KOH at a flow rate of 50 mL/min without pH control).

Exhibit 3.17. LEP of patterned membrane before and after DAC test.

Four Tubular Alumina Membranes	LEP (bars)	LEP (bars)after 138hours DAC test in pH>13	LEP (bars) after an additional 82-hour DAC test at 2wt%KOH
500 µm Grid Pattern	3.5	3.5	3.5

3.2 Developing an Electrochemical Solvent Regenerator for pH-swing assisted DAC

Evaluation of Electrodes for the Electrochemical Regeneration Cell and Depolarization

In order to develop the solvent regenerator, the initial experiment set involved electrochemical characterization in selecting electrodes that maximize current for a given voltage. Electrochemical tests were performed using a three-electrode cell configured with test working electrodes (i.e., electrode under examination) including platinum (Pt), graphite, stainless steel 304, and Nickel-Copper (Monel™). A saturated calomel electrode (SCE) and a titanium mesh were used as the reference and counter electrodes. The half cell is shown in **Exhibit 3.2.1a**. All three electrodes were connected to an Autolab PGSTAT128N potentiostat. In order to investigate the capability of the working electrodes for the hydrogen evolution reaction coupled with regenerating the caustic solvent and oxygen evolution coupled with proton production/hydroxide consumption for CO_2 evolution, cyclic voltammetry was conducted at 0.5 mV/s in a 40 mL mixture of 5% K_2CO_3 and 2.5% $KHCO_3$ as electrolyte at potential windows between -1.5 and +1.5 V vs. SCE. **Exhibit 3.2.1b** summarizes the results. For the cathodic reactions (hydrogen evolution), at a voltage of -1.5 V, Pt showed the best performance (most negative current), with performance in the order of Pt > Ni-Cu > 304 > Graphite. On the anode side (oxygen evolution), at +1.5 V, the performance was in the order of graphite> Ni-Cu > 304 > Pt. However, it should be noted that these anodic potentials may

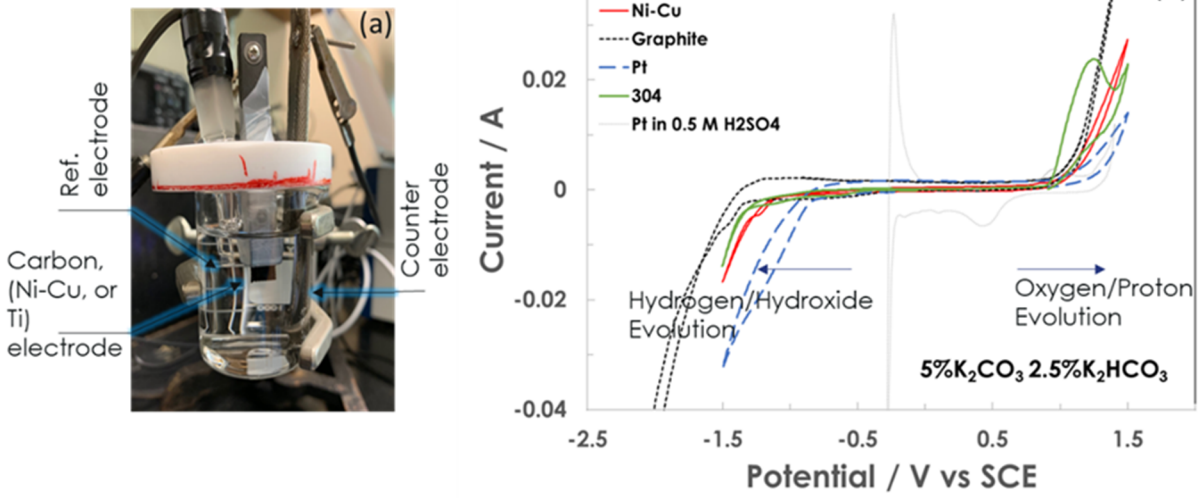

Exhibit 3.2.1. Half cell setup (a) and cyclic voltammogram (b) of test electrodes for electrochemical cell construction.

be coupled with the onset of material dissolution. Ni-Cu was selected for initial testing in the flow cell by considering a combination of its sufficient cathodic and anodic performance.

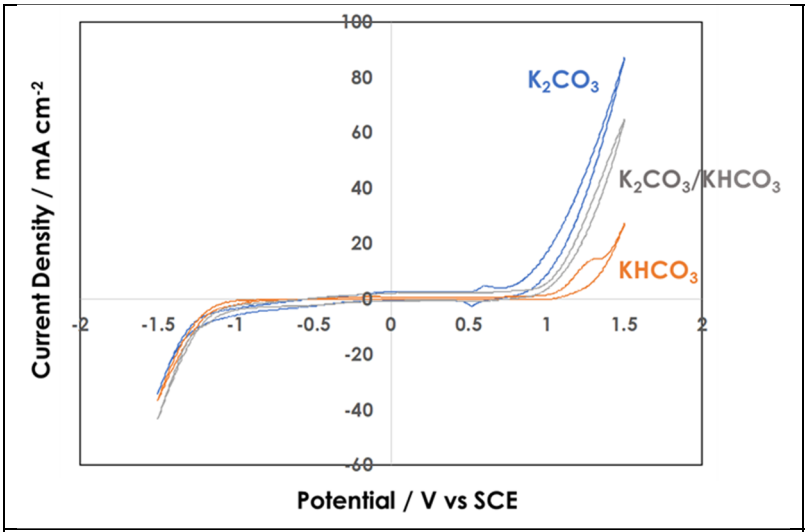

Exhibit 3.2.2. Cyclic voltammogram under different electrolyte compositions for electrochemical cell optimization.

Using the same setup, in order to investigate the electrochemical behavior of the Ni-Cu under different carbonate solvent speciation that can exist during electrochemical regeneration of the capture solvent and up-concentration of CO_2, cyclic voltammetry was conducted at 100 mV/s in K_2CO_3, $KHCO_3$, and a 50:50 mixture of both compounds at potential windows between -1.5 to +1.5 V vs. SCE. The concentration of K^+ was maintained at 0.07 M for the tests, and the cell temperature was 50 °C. **Exhibit 3.2.2** shows the resulting voltammograms. For the cathodic branch (hydrogen evolution), at a voltage of -1.5 V, only minor differences in current density were observed as water activity drives this reaction ($2H_2O + 2e^- = H_2 + OH^-$). In comparison, on the anode branch (oxygen evolution), at +1.5 V, the current density performance was in the order of K_2CO_3 > K_2CO_3 + $KHCO_3$ > $KHCO_3$, suggesting that increased OH^- activity drives this reaction ($4OH^- = O_2 + 2H_2O + 4e^-$). Furthermore, the results also indicated that larger overpotentials would be required to drive the electrochemical flow cell as the concentration of $KHCO_3$ increases in the system at the anode.

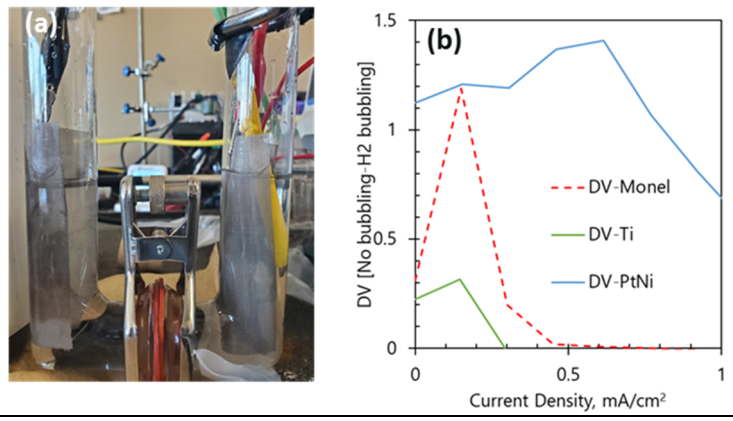

Exhibit 3.2.3. Electrochemical H-cell assembly (a) and depolarization response with Monel (Ni-Cu), Titanium (Ti), and platinum-Nickel (Pt-Ni) electrodes (b).

In order to demonstrate the capability and benefits of cell depolarization by substituting water electrolysis (hydrogen evolution on the cathode plus oxygen evolution on the anode) for a combination of hydrogen evolution and hydrogen oxidation reactions, thereby saving on energy requirement, an electrochemical H-cell (**Exhibit 3.2.3a**) was configured for depolarization operation. Carbonate electrolysis was performed in the H-cell with 50 mL 1% K_2CO_3 as the anolyte and catholyte with the anode and cathode compartments separated by a Neosepta CMX cation exchange membrane. The active membrane area was 5 cm^2. Electrodes including Ni-Cu/Ni-Cu,

Pt-Ni on Ni-Cu/Ni-Cu, and Ti/Ti were tested as anodes/cathodes to explore differences in electrode requirement under depolarized/non-depolarized modes. The nominal active area for the electrodes was 39 cm^2 which was used to determine current density. A purge line was also added to the anode chamber from a deionized H_2O electrolyzer operated at 1 A to supply H_2 for depolarization. Experiments were conducted with/without H_2purge to the H-cell's anode, and cell polarization was achieved with a power supply (Keithley 2450) by scanning the current and measuring voltage. **Exhibit 3.2.3b** shows the voltage difference between the non-purged and H_2 purged modes of operation as a function of current to assess voltage savings. The Pt-Ni electrode sustained a better depolarization performance than the Monel (Ni-Cu) and Ti electrodes. The investigation concluded that Pt-based electrodes were required for depolarization.

Electrochemical Regeneration Flow Cell

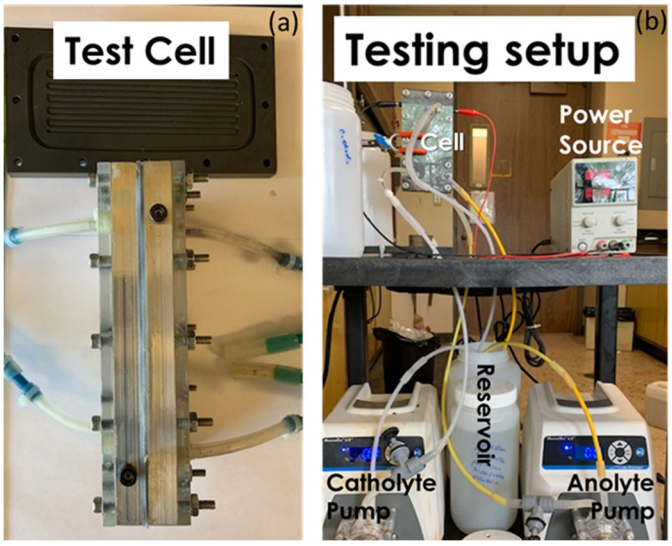

Exhibit 3.2.4. Electrochemical setup for carbon capture solvent regeneration and CO_2 release.

The selected electrodes were incorporated into flow cells as anode and cathode for continuous mode non-depolarized testing. The electrochemical flow cells were formed with a cation exchange membrane (Nafion), sandwiched by Monel (Ni-Cu-based) mesh as electrodes and graphite or stainless steel with embedded serpentine flow channels as current collectors and plastic endplates with inlet-outlet ports (**Exhibit 3.2.4 (a)**). The flow cell is incorporated into the test setup shown in **Exhibit 3.2.4 (b)** to facilitate testing where two pumps independently circulate the test solution from the reservoir via the cathode and anode compartment of the cell while a potential or current is applied to the cell via the power source.

UK CAER evaluated caustic capture solvent electrochemical regeneration using the setup from **Exhibit 3.2.4** and a feed solution prepared from a mixture of 5% K_2CO_3 and 2.5% $KHCO_3$. The solvent was circulated as anolyte and catholyte at 4.3 mL/min in a single pass, while the cell was polarized in constant current mode with test currents ranging from 0 to 7 Amps to control the loading factor, $L_F = \frac{i}{K^+QF}$, where i, K^+, Q, and F are the current, total K^+ ion concentration, flow rate, and Faraday's constant, respectively. When $L_F > 1$, the K^+ transport can no longer support the ionic current, leading to an increased crossover of H^+ to the cathode to recombine with generated OH^- ions, reducing KOH formation efficiency for capture. Alkalinity [$2CO_3^{2-} + HCO_3^- + OH^- - H^+ \approx K^+$] and pH measurements performed ex-situ were used to evaluate the performance of the electrochemical regenerator, and the results from the measurements are shown in **Exhibit 3.2.5**.

In summary, as the loading factor increases, (a) the pH decreases at the anode, but increases at the cathode, suggesting proton generation/hydroxide consumption (oxygen evolution) at the anode and hydroxide production (with hydrogen evolution) at the cathode, and (b) alkalinity decreases at the anode, but increases at the cathode, consistent with potassium transfer from the anode to the cathode via the cation-selective membrane and driven by the applied current. The results show that the regenerator cell produced near pH 14 (~ 1M KOH) capture solvent for direct capture.

When the ERC is electrically polarized, the input current/charge is balanced by charge transport and electrochemical reactions, including O_2 and H_2 evolutions. The ERC's anode to cathode K^+ transport efficiency, derived from alkalinity difference normalized by current, was further explored at different loading numbers, concentrations, and compositions. **Exhibit 3.2.5c** shows that as the loading factor increased, the K^+ transport efficiency decreased, consistent with increased protons

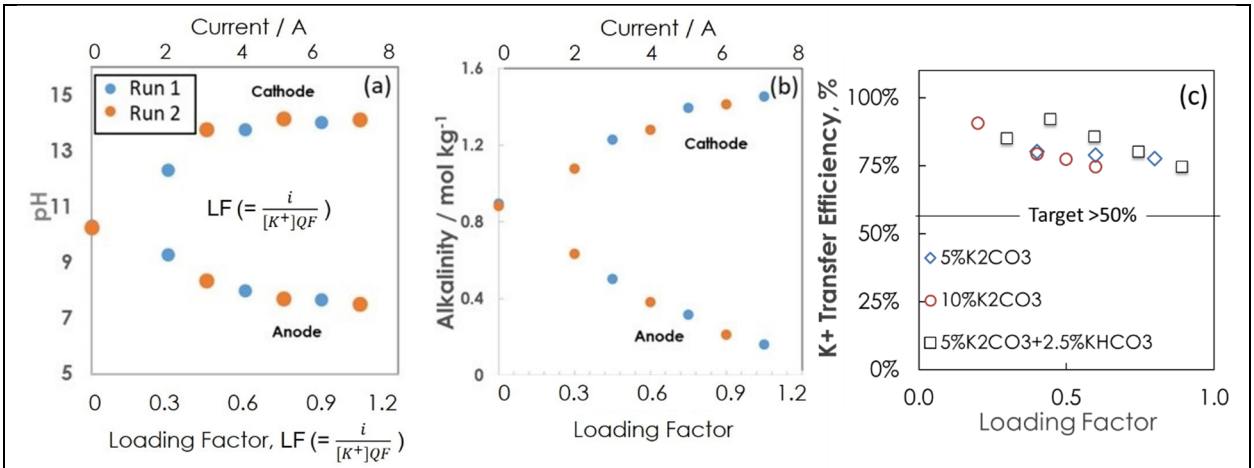

Exhibit 3.2.5. Effect of loading factor on pH (a), alkalinity (b), and potassium transfer efficiency (c) for the electrochemical regenerator.

crossover at high loading factors. Nevertheless, transport efficiency was maintained above 70% for the census of test conditions compared to the project's target of 50%.

In a further characterization of the ERC, gas side analysis was used to examine the efficiency of gas evolution from the anode as a function of flow rate, which is inversely proportional to the loading factor. The feed solution was 10% K_2CO_3. The cathode flow rate was maintained at 8.6 mL/min while the anode flow rate was varied. Sensors for O_2, CO_2, and pH were connected in-line to monitor the process, and experiments were performed at a constant current of 4 A. **Exhibit 3.2.6(a)** shows the response of pH and voltage during operation. As flow rate increases (loading decreases), anode pH swing is larger (e.g., pH swings from ~12.3 to 9.5 at 4.1 mL/min but 10.5 at 10.4 mL/min) while voltage requirement is smaller (e.g., 8.3 V at 4.1 mL/min vs. 7.3 at 10.4 mL/min). As expected, the higher molar influx of the carbonate solution at higher flow rates can buffer the proton generation/hydroxide consumption rate set by the input current, leading to a weaker pH swing response. **Exhibit 3.2.6b** shows the cell's molar rate for O_2 and CO_2 effluent. At 4 A operation, the expected O_2 molar rate is 0.62 mmol/min [N (mol/s) = Current/(4*Faradays constant)], and **Figure 3.4.1b** suggests that O_2 efficiency is ~100%, which implies CO_2 release is chemical equilibrium controlled. The Exhibit also shows an increased CO_2 evolution rate at lower anolyte flow rates (higher loading factor), consistent with the pH trend observed in **Exhibit 3.2.5a**

since increased acidity at the anode enhances CO_2 evolution in the analyte.

Furthermore, as pH decreases, the molar concentration of bicarbonates is expected to increase, causing voltage requirement to increase, consistent with **Exhibit 3.2.2**. However, it should also be noted that higher flow rates also independently reduce voltage requirements by helping liberate bubbles that accumulate at the electrode-electrolyte interface and separate the electrode from the electrolyte within the cell. For the cell employed here for testing, the anode and membrane were separated by a 6mm wide flow space, which increased the ohmic overpotential of the system. By reducing the spacing to 1.5mm, the operating voltage reduced from 8.3 V at 4.1 mL/min (6mm) to 6.8 V at 4.1 mL/min (1.5mm). The pH drop remained similar, dropping from ~12.3 to 9.5 at 4.1 mL/min.

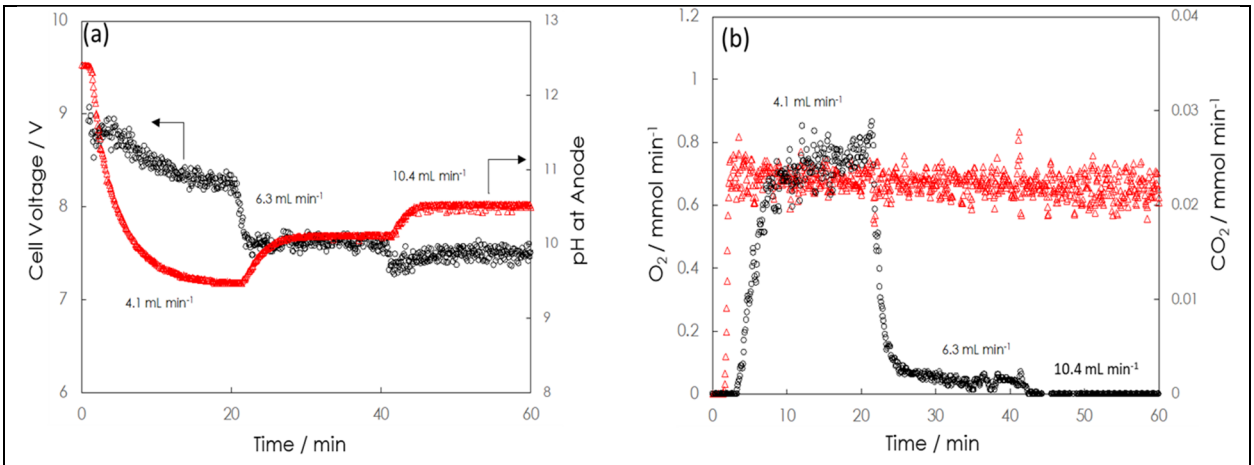

Exhibit 3.2.6. Effect of flow on pH and voltage (a), and effluent O_2 and CO_2 response during polarization at 4A.

Depolarization of the Electrochemical Regeneration Flow Cell

During the initial experiments performed with the H-cell (**Exhibit 3.2.3**), H_2 was directly bubbled into the anode chamber to facilitate depolarization, suppressing ~1 V when a Pt-metal catalyst group was employed. However, since bubbling H_2 into the analyte storage tank will be limited by H_2 solubility, a three-compartment ERC was designed, as shown in **Exhibit 3.2.7(a)** and used to demonstrate depolarization under flow conditions. The cell includes a gas compartment next to the anode separated by a Porex membrane, and the anode, in turn, annexes the cathode separated by a cation exchange membrane. The cell configuration facilitates an easy switch to a non-depolarized operation by simply isolating the gas compartment via valves. H_2 was supplied from an external electrolyzer operated at 1-5 A. Experiments were conducted with/without H_2 purging the cell anode, and polarization was achieved with a power supply (Keithley 2450) by scanning the current and measuring voltage. **Exhibit 3.2.7(b)** shows polarization curves for the non-purged and H_2 purged modes of operation as a function of current to assess voltage savings. Whenever H_2 was purged, the voltage was suppressed by ~1.4 V. Impedance spectroscopy was used for further analysis at open circuit conditions at 10 mV RMS and frequencies from 50 kHz to 50 mHz, determining the cell's ohmic resistance of ~3 ohms. The ohmic resistance was used to compensate for the voltage requirements and similarly plotted in **Exhibit 3.2.7b.** The ohmic compensated polarization plot confirmed a smaller voltage requirement and reaction overpotential with depolarization, and a significant portion of the voltage requirement was ohmic as the applied current/loading factor increased.

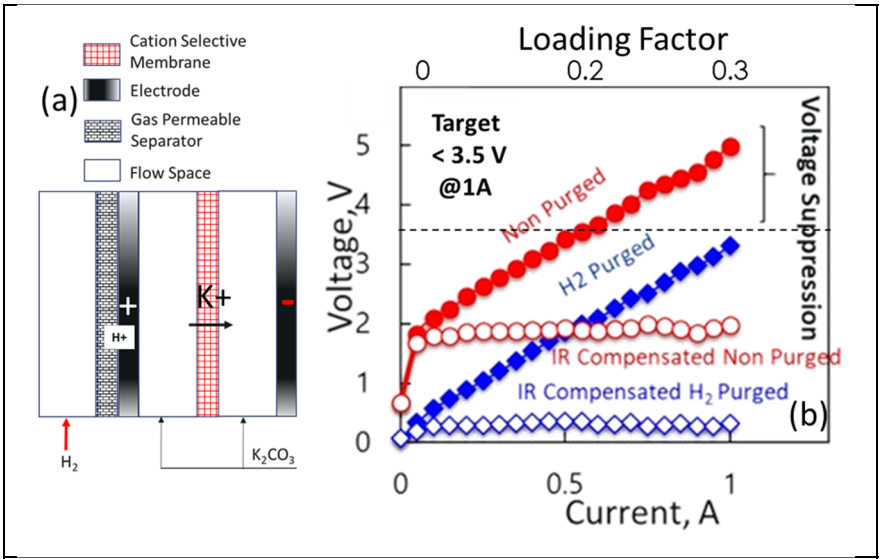

Exhibit 3.2.7. Cell configuration (a) and Polarization response (b)for flow cell operation with and without depolarization in 0.1 M carbonate solution as the anolyte and catholyte, circulated at 10 mL/min. The cathode was Monel, and the anode was respectively catalyst-coated Monel.

Under similar test conditions, the CO_2 and O_2 release performance at the anode were further examined with and without depolarization. The O_2 and CO_2 molar rates are shown in **Exhibit 3.2.8**. With depolarization, while there was CO_2 in the effluent, the results show no oxygen response in the system until a higher current, where anode H_2 concentration polarization is suspected and accounts for the deviation in the CO_2 trend in the **Exhibit 3.2.8b**, where the CO_2 rate becomes asymptotic to the x-axis. This set of results shows that in addition to a lower voltage operation, oxygen-free CO_2 can be obtained by depolarizing the anode.

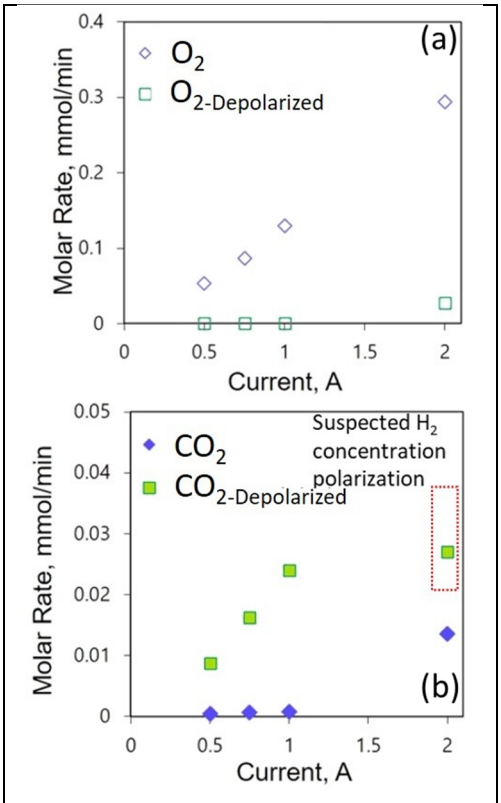

Exhibit 3.2.8. The release of Anode O_2 and CO_2 depolarization operations.

Since the anode employs H_2 for depolarization, the H_2 utilization performance needs to be addressed. In a separate experiment, H_2 utilization during depolarization was explored with H_2 generated from an external electrolyzer fed to the anode of the ERC at different rates. A gas flow meter (Aalborg) downstream on the anode measures the gas flow rate. In addition to mass balance analysis facilitated via in-line gas sensors (Vernier, carbon dioxide and oxygen), H_2 concentration was also evaluated using an SRI Gas Chromatograph. **Exhibit 3.2.9** compares the theoretical and measured H_2 utilization as a function of the ERC current.

For the theoretical calculation symbolized by the guidelines, the regenerator current is normalized by the external electrolyzer current, e.g., for an external electrolyzer supplying hydrogen at 4 Amps to a regenerator operated at 2 Amps, the theoretical (or maximal) faradaic utilization is 50%. **Exhibit 3.2.9** shows the utilization of hydrogen fed to the regenerator at 4 A (~28 mL/min H_2) and 10 A (~70 mL/min H_2). A maximal

of ~50% utilization was achieved during the 4 A H_2 feed to the regenerator. Deviations from the theoretical utilization lines are observed as the ERC's current increases, which may be consistent with an inhibiting response from the
competition with the oxygen evolution reaction [3].
In addition to depolarization, this cell configuration facilitates an easy switch to a non-depolarized operation by simply closing off the gas compartment via valves. However, considering that the electrode is in direct contact with the solution, a flooded electrode can restrict hydrogen transport to the triple-phase boundary, as shown by the flattening of the H_2 curve in **Exhibit 3.2.9**. Nevertheless, it should be considered that the effluent gas may yet be further utilized by a downstream fuel cell for energy production, and other cell assemblies can be designed to improve utilization.

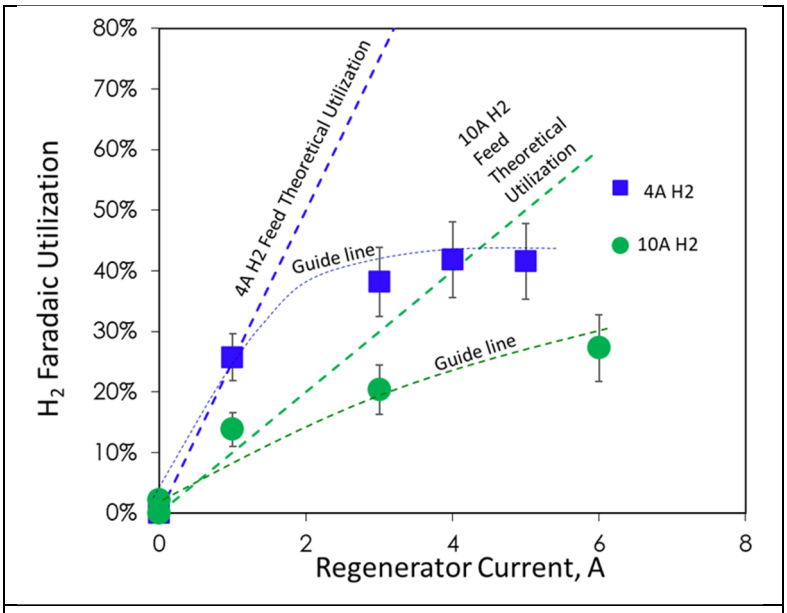

Exhibit 3.2.9. Faradaic utilization during depolarization operation with hydrogen fed to the regenerator at 4 A and 10 A.

3.3 Integrated System for Direct Air Capture

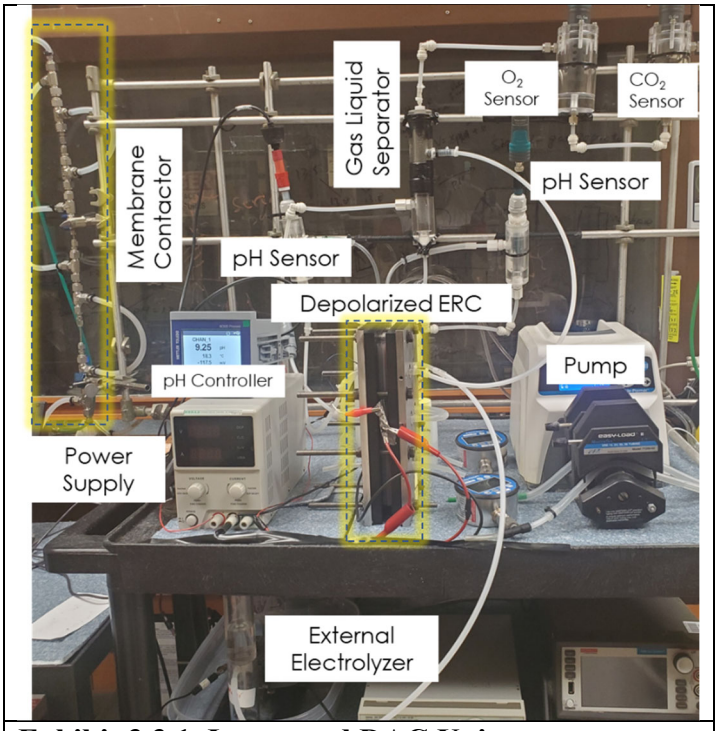

Exhibit 3.3.1. Integrated DAC Unit.

UK CAER integrated the ceramic membrane contactor and depolarized electrochemical cell for CO_2 capture and solvent conditioning. **Exhibit 3.3.1** shows a picture of the integrated unit, including the MC, ERC, and auxiliaries. A semi-continuous approach was employed to facilitate testing where the solvent was first conditioned by the electrochemical regenerator cell, followed by recirculation in the contactor shell for capture, during which the regenerator remained off. The capture fluid and anolyte were prepared from 180g of 15 wt% K_2CO_3. **Exhibit 3.3.2a** shows the voltage and energy profile in the regenerator. The regenerator cell was operated in constant current mode at 0.5 A with excess hydrogen externally supplied at 3A. The nominal voltage was 1.1 V and

effective charging required < 1 hour, resulting in ~315 J to boost the pH via $2H_2O + 2e^- \rightarrow H_2 + 2OH^-$ from ~12.2 to 12.6.

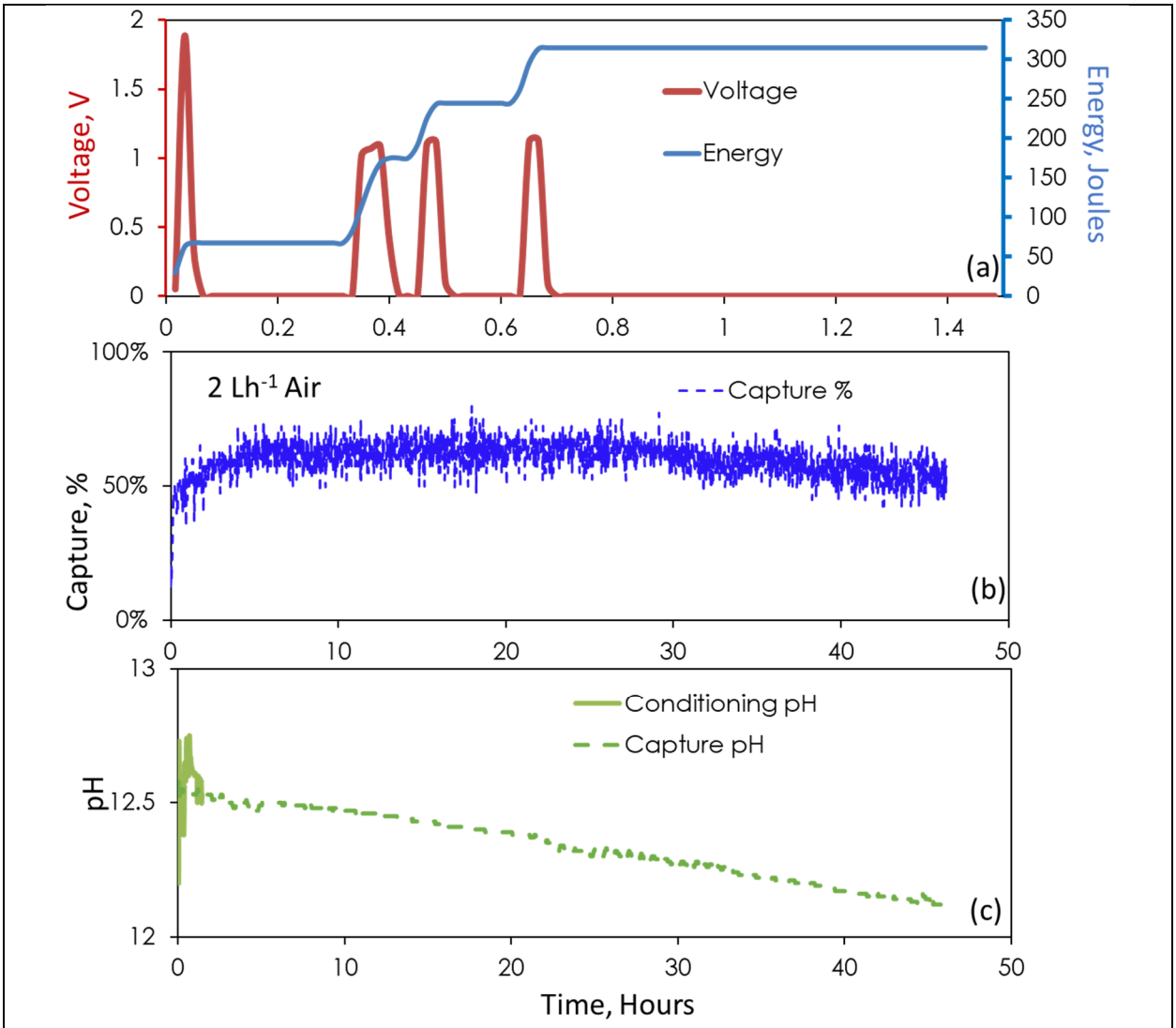

Exhibit 3.3.2. Performance of integrated system for DAC and solvent regeneration including voltage and energy profiles (a) % capture (b), and pH profiles (c).

The membrane contactor consisted of four serial ceramic membranes with air (400 ppm CO_2) influent on the tube-side of the membrane at 2 L/hr, corresponding to a gas residence time of ~5 s. Their geometric area was 62.3 cm^2. **Exhibit 3.3.2b** shows a nominal capture of 60% (~160 ppm CO_2 in effluent) was maintained during the testing period (46 hours). Since CO_2 is captured via $CO_2 + 2OH^- \rightarrow CO_3^{2-} + H_2O$, a pH probe also tracks the capture performance, and pH gradually decreases with time as more CO_2 is loaded into the solvent (Exhibit **3.3.2c**). By integrating the CO_2 curve with respect to the starting CO_2 value of 400 ppm, 9 x 10^{-4} moles of CO_2 was captured during the testing period, leading to the energy requirement of ~350 kJ/mol CO_2. After testing, the solvent was collected for inductively-coupled plasma analysis compared to the starting solution. **Exhibit 3.3.3** shows the solvent analysis after DAC testing, including the RCRA metals Cr, As,

Se, Cd, Ba, and Pb. All tested metals were below the RCRA classification for hazardous waste. Platinum was also tracked to determine anode stability and showed only a marginal increase in the anode. Trace metals in the water are presumed to originate from trace impurities in the chemicals used, with some contributions from the electrodes. Summarily, results from the solvent analysis alleviated concerns about materials stability and waste disposal at the current scale. Furthermore, it is considered that depolarization abets electrode degradation reactions, enhancing the stability of the DAC unit.

Exhibit 3.3.3. Analysis of Solvent after DAC Testing.

Samples	Cr (ppb)	As (ppb)	Se (ppb)	Cd (ppb)	Ba (ppb)	Pt (ppb)	Pb (ppb)
Raw/Feed	5.50	0.39	2.67	0.47	276.64	0.06	13.14
Cathode	14.30	0.52	2.69	0.11	889.90	1.90	19.19
Anode	1.16	0.42	2.02	0.09	396.50	3.02	84.69
RCRA	5000	5000	1000	1000	1E05	NA	5000

3.4. Environmental Safety Assessment for Integrated Process

ALL4 completed an Environmental Health and Safety (EH&S) Assessment for the integrated process developed by the University of Kentucky for directly capturing CO_2 from the air. Experimental testing was conducted at the UK CAER facility in Lexington, Fayette County, Kentucky. Data obtained was extrapolated to evaluate the impact of a comparable system for a commercial scale (estimated to have a multiplier factor of 10,000).

The purpose of the EH&S Assessment was to determine if any unacceptable environmental, health or safety concerns may prevent the implementation or environmental permitting of the technology evaluated at the bench-scale and evaluate whether there may be any unacceptable environmental, health or safety concerns that would prevent implementation, or environmental permitting of a commercial scale DAC system with the technologies evaluated. The assessment included reviewing process flow diagrams, input and output flow rates for primary materials, literature describing similar processes and chemicals used or created during the process, actual air emission and wastewater test data and air emission calculations. The evaluation included the identification of risks related to hazardous chemicals, air emissions, wastewater discharges, solid wastes generated and employee hazards.

The assessment did not identify any obvious concern for the bench-scale operation and no apparent barriers to implementation at a larger scale. Including hydrogen generation, processing and storage for use as a fuel or source for fuel cell electrolysis at a commercial scale would involve more extensive safety precautions in equipment design, operation and storage facilities; however, these aspects are not unique and can be managed safely and efficiently following established and emerging standards. Additional testing at a larger scale was suggested to better quantify air emissions and potential waste issues derived from a commercial scale system.

This project generated approximately 250 mL of spent capture solvent. This material was not identified as hazardous waste. A commercial facility may be anticipated to generate approximately

2,500 L (~660 gallons or twelve 55-gallon drums) of spent capture solvent that would not be routine and likely only be generated at decommissioning.

There were few hazardous chemicals used in the project, the primary hazard being potassium hydroxide, a corrosive chemical used as a carbon capture solvent. Potassium carbonate can be a skin, eye, and respiratory irritant in powder form. Fire hazards existed due to the wide flammability range of hydrogen produced to a varying degree in the solvent regeneration process. These are not unusual materials or hazards. Appropriate protective equipment and measures are needed to prevent injury from exposure.

A primary concern for commercial-scale operations would involve effective hydrogen production and storage management. The design for the regenerator should emphasize the isolation of hydrogen from oxygen and potential ignition sources, good ventilation and installation of appropriate monitoring and warning systems with automated shut-down protocols. National and international standards have been established and can be used to address these recommendations (e.g., NFPA 2 and other NFPA standards, ANSI/AIAA G-095A-2017 and ISO/TR 15916).

4) CONCLUSION

UK CAER's DAC system comprises an ERC and MC working synergistically to (1) directly remove CO_2 from air; (2) produce H_2 for sale, energy storage, grid-management, and depolarization to directly reduce the energy requirement for DAC; and (3) avoid high-temperature requirement while simplifying water management and integration with renewable energy storage like solar cells. The project results verified that UK CAER's integrated approach addressed the complexities of incumbent DAC systems by demonstrating at ambient conditions, including (1) low gas-side pressure-drop facile CO_2 capture via a membrane contactor with in-situ generated hydroxide as capture solvent, (2) multi-functional electrochemical regenerator for hydroxide regeneration, CO_2 concentration and ultra-pure H_2 production after dehumidification, and (3) depolarization using cathode-produced $H_2$to reduce energy requirement that can be applied during peak energy demand. When depolarization is employed, the operating voltage is reduced by more than 1 V, and capture was demonstrated at an energy requirement of ~350 kJ/mol CO_2. An EH&S Assessment was performed on the process and did not identify any concern for the bench-scale operation and no apparent barriers to implementing UK CAER's carbon capture and solvent regeneration system at a larger scale.

5) AREAS OF FUTURE INTEREST

UK CAER developed a simple two-unit operation yet effective DAC technology through this project. In order to advance this methodology, the following areas have been identified as "important" for the next step:

1 *Reactor design and new electrodes to suppress the impact of bubble on over-voltage*. Under our underlying process, gas bubbles, including hydrogen on the cathode and oxygen on the anode, are continuously produced in the ERC, although it should be noted that depolarization mitigates oxygen evolution. These gas bubbles can coalesce to separate the liquid solvent from the solid

electrode leading to high resistance in the ERC. Mitigation approaches include (1) increasing the solvent flow rate to convectively transport gases out of the system and refresh the electrode surface, (2) applying sonication/pulses and (3) high-pressure operation to ensure the gas bubble remains dissolved during operation but adds cost to the process. Conversely, new cell designs and electrodes can be explored to mitigate these losses by tuning the interfacial tension of the solid-liquid-gas interfaces.

2. *Customization for End-Use*. Another consideration is the composition and end-use of the anode gas exhaust, including CO_2, CO_2/H_2 and CO_2/O_2. This project found the anode exhaust customizable based on the ERC cell configuration and operation. While high purity CO_2 is preferred, some gas mixtures can be used for molten carbonate fuel cells (CO_2/O_2) or polymer electrolyte fuel cells (CO_2/H_2). Furthermore, the ability for the direct electrochemical conversion of CO_2 in these streams to higher hydrocarbons and useful chemicals is gaining interest as a part of direct air capture and utilization.
.

6) LIST OF EXHIBITS

7) ACKNOWLEDGEMENTS

The completion of this project leveraged organizational participation between UK CAER and ALL4 Inc. The authors of this report would like to acknowledge the contributions of Keemia Abad (UK CAER) for sample analysis and Roger Perrone (UK CAER) for the fabrication of the electrochemical regeneration cells and reactors, Emmanuel Ohiomoba (UK CAER) for helping with experiments, and ALL4 Inc for developing a detailed EH&S Assessment.

8) REFERENCES

1. Fan, P., Pan, R., & Zhong, M. (2019). Ultrafast laser enabling hierarchical structures for versatile superhydrophobicity with enhanced Cassie–Baxter stability and durability. *Langmuir*, *35*(51), 16693-16711.
2. Jani, J. M., Wessling, M., & Lammertink, R. G. (2012). A microgrooved membrane based gas–liquid contactor. *Microfluidics and nanofluidics*, *13*(3), 499-509.
3. Vos, J. G., & Koper, M. T. M. (2018). Measurement of competition between oxygen evolution and chlorine evolution using rotating ring-disk electrode voltammetry. *Journal of Electroanalytical Chemistry*, *819*, 260-268.

9) LIST OF ABBREVIATIONS AND ACRONYMS

DOE - Department of Energy
DAC – Direct air capture
DEC – Depolarization electrochemical cell
ERC – Electrochemical regeneration cell
EDEMS - Enhanced depolarized electro-membrane system
MC – Membrane contactor
PI – Principal investigator
SMG – Smith Management Group
TRL - Technology Readiness Level
TMP – Technology Maturation Plan
UK CAER - University of Kentucky Center for Applied Energy Research